Behaviour of GFRP Prestressed Concrete Straps

By

Yasmine El-Sayed

A Thesis

Submitted to the Faculty of Graduate Studies of

The University of Manitoba

In Partial Fulfillment of the Requirements for the Degree of

Master of Science

Department of Civil Engineering

University of Manitoba

Winnipeg, Manitoba

ABSTRACT

Steel straps are being used for confinement purposes of steel-free bridge deck slab. The objective of this study was to use GFRP prestressed concrete straps as an alternative to steel straps, and assess the effect of the alkaline concrete environment on the long-term performance of GFRP. Each strap was 160 x100 mm^2 in cross section, 2000 mm in length and pre-tensioned with two 16 mm diameter GFRP strands. The experimental study included testing three sets of concrete straps, pre-stressed at 35%, 45%, and 55% of ultimate strength of GFRP. The straps were tested in tension after being subjected to temperatures from -25^{o}C to +40 ^{o}C in an environmental chamber. Another two sets of straps were cast and tested two and a half years later. The control and conditioned samples achieved comparable results proving that GFRP can withstand prestressing levels higher than 25% and up to 35% of their ultimate strength.

Acknowledgements

I would like to offer my sincere appreciation to my advisors Dr. Aftab Mufti and Dr. Dagmar Svecova for their continuous guidance and support throughout my research. I am eternally grateful for their professional encouragement and technical guidance even though there were many obstacles encountered during the course of the project. They have introduced me to a new branch in structural engineering, being the pioneers in the area of FRP design. This research helped me develop evolve as a person and as a researcher.

I am grateful for the financial support of grants from the Canadian Centres of Excellence on Intelligent Sensing for Innovative Structure, ISIS Canada in providing these grants.

For their assistance during the experimental program research, I would like to thankfully acknowledge the staff at the McQuade Structures laboratory: Mr. Chad Klowak, Mr. Grant Whiteside and Dr. Liting Han. I wish to also thank my fellow graduate students for their help and support during my Master's program.

My final thanks goes to my friends and family for always being there for me, especially my parents for their constant encouragement and blessings; I owe them all my accomplishments. I am eternally grateful to my husband, Nashaat Soliman, and my son, Haddy, for being my pillars of strength.

Dedication

My Parents Enas Samaha and Dr. Magidy El-Sayed

My Pillars of Strength my husband Mohammed Soliman and our son Haddy Soliman

TABLE OF CONTENTS

LIST OF FIGURES

LIST OF TABLES

List of Acronyms

CHBDC	Canadian Highway Bridge Design Code
CFRP	Carbon Fibre Reinforcing Polymers
FRP	Fibre Reinforcing Polymers
GFRP	Glass Fibre Reinforcing Polymers
OHBDC	Ontario Highway Bridge Design Code

List of Symbols

A	Area of strap
A_c	Area of concrete
A_{frp}	Area of FRP
Δ	Axial deformation

E	Modulus of elasticity of concrete
E_f	Modulus of Elasticity
E_{ff}	Ultimate strain in tension
$\Delta\varepsilon_p$	Strain difference
ε_c	Strain in concrete
ε_p	Strain in prestressing reinforcement
ε_{pbed}	Strain in pre-tension bed
ε_s	Strain in reinforcement
F	Factor based on the position of the panel
f_c	Stress in Concrete
f'_c	Peak stress obtained from a Cylinder Test
f_{sp}	Splitting Strength
f_p	Stress in prestressed reinforcement
f_u	Ultimate tensile strength
L	Length of the member
N	Applied load
P_u	Ultimate pullout load
S	Spacing of supporting beams
S_1	Spacing of straps
r_o	Radius of GFRP bar
r_1	Radius of Concrete cylinder equivalent to minimum concrete cover

t	thickness of the deck slab
v	Poisson's ratio

Chapter 1

Introduction

1.1 General

About 41% of the bridges in the USA and Canada are over 40 years old and are classified as deficient and in need of rehabilitation or replacement (Sohanghpurwala, 2006). There are various factors causing the deterioration in bridges, such as the low load carrying capacity of the bridges as they were designed for much lower traffic volumes, smaller vehicles and smaller loads. The freeze thaw cycles with the use of de-icing salts are the main causes of the severe corrosion that the bridges experience. In addition, these bridges have not been adequately maintained.

Steel-free bridge deck slab is an alternative to the conventional deck slab, as no internal reinforcement is placed in the decks, so the problems of deterioration, corrosion and delamination will not occur. Since the cost of maintenance required for corrosion will no longer be required, the steel-free bridge deck slab is considered an economical solution.

The confinement provided in the steel-free bridge deck slab in both the transverse and the longitudinal direction provides the deck slab with its strength by developing the arching-action in the deck slab. In the presence of a load, a longitudinal crack appears in the deck slab between the girders, aiding in the development of the arching action. The transverse confinement is provided with the means of developing the arching action by a number of steel straps (50x25 mm) welded to the top flanges of the girders preventing the lateral movement of the top of the flanges whereas, the longitudinal confinement is provided with the means of shear studs welded to the top of the girders. The strength of the system depends on the stiffness of the straps and not on their strength.

The steel straps providing the transverse confinement may face corrosion. An alternative for confinement, prestressed GFRP concrete straps (150x100 mm) has been developed as

an external transverse confinement (Banthia, 2003). Prestressing the GFRP provides the concrete with the ability to crack at a higher load. This property provides the strap with higher stiffness to overcome the tension due to applied loads on the steel- free bridge decks. The concrete straps when used in the steel-free bridge deck slab have been shown to have twice the stiffness as that of steel straps. The durability of the prestressed concrete straps under environmental conditioning needed to be tested.

The main focus of this study is to understand the effect of different prestressing levels on the stiffness of the straps as well as on their durability.

1.2 Objectives of the Project

- To find the maximum safe level of prestressing for GFRP prestressed concrete straps.

- To investigate the effect of freeze – thaw cycles and repeated loading on the behavior of GFRP prestressed concrete straps.

1.3 Scope of the Project

- Only GFRP reinforcement will be investigated.

- Three prestressing levels of 35%, 45% and 55% of the ultimate strength of GFRP will be used.

Chapter 2

Literature Review

2.1 Steel-Free Bridge Deck Slab

2.1.1 History

Steel reinforcement faces corrosion problems which require high maintenance and rehabilitation costs. These problems arise during winter, when fluctuation in temperature occurs and de-icing salts, the main catalyst of corrosion, are extensively used. The expansive corrosion property of steel can cause cracking and spalling within the concrete cover. Among the alternatives to overcome this problem have been steel reinforcements with protective coatings, increasing the depth of cover, and increasing the density of concrete mixes; all of these solutions have been deemed too costly and it is recognized that the same problem would re-occur with time.

With the complete removal of the internal steel reinforcement and with proper confinement methods of a concrete slab on a girder bridge deck, an internal arching action would develop when subjected to a concentrated load. The slab would fail in punching shear rather than flexure as the arching action contributes a compressive stress to the deck slab. (Hewitt & Batchelor, 1975; Beal, 1982; Fang, et al., 1986; Jackson & Cope, 1990). An innovative solution, a steel-free bridge deck slab, was introduced, thus completely eliminating the internal steel reinforcements to completely remove the cause of concrete deterioration (Mufti, et al., 1991). Furthermore, synthetic nonferrous reinforcing material was introduced, and the in-plane restraint was established by means of external steel reinforcement. Polypropylene, a fibre of low modulus of elasticity and relatively inexpensive and durable material, was used to provide some control over cracking due to shrinkage and temperature change (Mufti, et al., 1993). It should be noted

that the fibres act only as secondary reinforcement to control the cracking due to shrinkage during curing and to provide ductility to the hardened concrete.

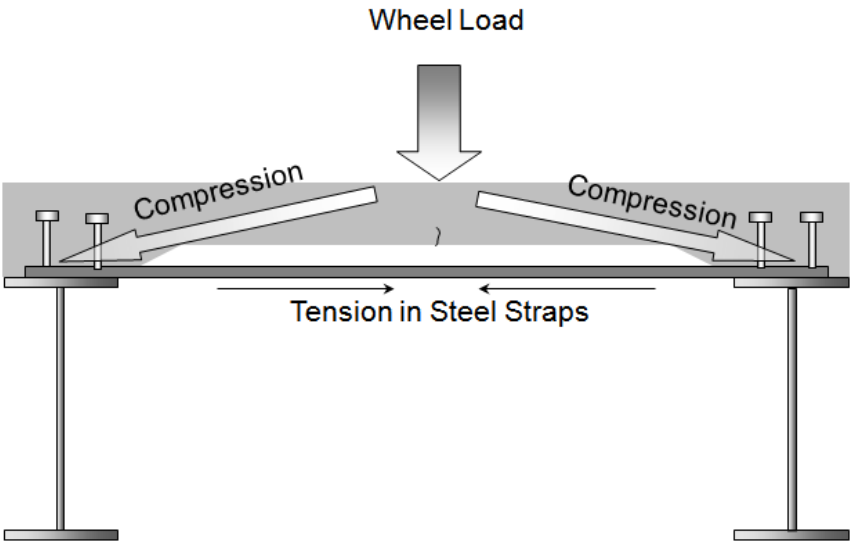

Figure 2.1 Steel-free bridge deck slab confined using steel straps

Both longitudinal and transverse confinements of the deck slab define the load carrying capacity of the deck slab. Transverse confinement restrains the top of the girders from moving laterally when the arching action is induced. This transverse restraining action can be provided by either transverse bottom bars embedded in concrete or by external steel straps lying outside the concrete slab and welded to the top of the girders as seen in Figure 2.1. The deck slab fails in punching, at a higher load than in flexure; hence, less reinforcement would be required, resulting in considerable savings. The Ontario Highway Bridge Design Code (OHBDC, 1979), for instance, evidenced improved behaviour, and later in 2000 the Canadian Highway Bridge Design Code (CHBDC 2000) introduced an entire chapter on Fibre Reinforced Concrete (FRC) using the arching action system, (Mufti, et al., 1993)

.

2.1.2 Actual loads experienced by Bridge Deck Slab

Researchers have been interested in studying the actual maximum wheel loads, bridge deck slab experience. It has been observed that the maximum wheel load in Japan is 313 kN (Matsui, *et al.* 2001). On the other hand Mufti, et al. (2002) researched the maximum lifetime axle load in Canada and concluded it to be 345 kN.

2.1.3 Steel-Free Bridge Deck Slab Constructed in Canada

The first bridge built to take into account the benefits of the arching action was the Conestoga River Bridge constructed in Ontario in 1975. At that time it was still believed that when the slab is subjected to a concentrated load it would fail in flexure. When the Conestoga River Bridge was designed, accounting for the arching action with girders spaced at 2 m, it required the use of 20 kg/m^2 of steel, which is about two thirds the quantity required in a conventional deck slab. The Conestoga River Bridge is still in service and is performing well (Bakht & Mufti, 1998).

The arching action could be produced by means of confinement in both the longitudinal and transverse directions. In the longitudinal direction, a composite action was initiated by means of edge beams with high flexural rigidity in the plane of the slab (Bakht & Agarwal, 1993). In the transverse direction, the confinement could be provided with bottom transverse reinforcement, or it could be entirely removed and replaced with external steel straps welded to the top of the girder. In such a case, the slab would be devoid of any reinforcement and so named as " steel-free" bridge deck slab (Bakht & Mufti, 1996).

In 1998, Bakht and Mufti reported that five steel-free bridge deck slab, each having a unique feature, had been built in Canada and were in service and in good condition.

2.1.4 Types of Transverse Confining Systems.

The CHBDC specifies that the transverse confining system of a steel-free bridge deck slab should be composed of straps, each having a minimum cross sectional area (*A*, mm^2), and can be calculated from the following formula:

$$A = (F_s \times S^2 \times S_1 \times 10^9) / (E \times t) \qquad \text{Equation 2.1}$$

Where F_s = 6.0 and 5.0 MPa for external and internal panels.
S is the girder spacing in m.
S_1 is the strap spacing in m and should not exceed 1.5 m.
E is the modulus of the strap material in MPa.
t is the slab thickness in mm.

The presence of the modulus of elasticity in the denominator verifies that the requirements for the strap emphasize stiffness rather than strength. The connection of the strap, directly or indirectly, to the girder is required to have strength of at least 200*A* in Newtons. In the case of steel straps the required connection has half the axial strength of the strap. There are several alternative methods for transverse confining as presented by Bakht and Lam (2000).

FRP, due to its high durability, can also be used as an external confining element. These bars are directly embedded into the deck slab haunch above the girders, and the restraint would develop through the bond of the FRP and the concrete. As it is not expected to face deterioration, no replacement would be required. Carbon FRP (CFRP) tendons are suitable in aggressive environments but are very expensive and suffer high prestressing loss as they have a much higher modulus of elasticity than that of concrete resulting with

a high stiffness ratio. On the other hand, GFRP is less expensive, and has a modulus of elasticity almost equal to that of concrete, so the material tends to suffer less prestressing losses.

Several researchers (Mufti et al., 1993 and Newhook & Mufti,1996) have measured the strain in the straps of a full scale model of a steel-free deck slab for a wheel load of 400 kN which led to a tensile force of 50 kN in the strap. They hypothesized that using concrete straps for external transverse confinement would result in the cracking being avoided by means of pre-tensioning. The prestressing of the straps would be provided by means of steel or FRP tendons. For design purposes, it could be assumed that the maximum tensile force in the concrete would be twice the experimental tensile force of 50 kN, and in order to prevent the concrete from cracking, it should be prestressed to have cracking load of at least 100kN.

Due to concerns about the GFRP's ability to handle high prestressing levels and due to the limited studies on durability in a concrete environment under high stresses, the CSA S806 (2002) articles 10.5.1 and 7.1.2.3 have limited the prestressing levels to 23% of its ultimate strength. Banthia (2003) believed that stressing limits in the code undermines the material's ability to handle higher stresses and so he studied the possibility of prestressing GFRP to 45% of its ultimate strength as an application of straps to be used in steel-free bridge deck slab.

Banthia (2003), studied the feasibility of using the GFRP prestressed concrete straps for transverse confinement of steel-free decks slabs, as seen in Figure 2.2. The straps were 150x100 mm, each with 2 GFRP bars 15 mm in diameter and prestressed at 45% of their ultimate strength. The primary concern for using these structural elements is their axial stiffness; hence, the straps were first subjected to 50 cycles of 50 kN, and then tested to failure reaching an ultimate load of 250 kN. The straps did not crack until a load of nearly 170 kN; the behaviour of the straps remained linear. The stiffness of the GFRP pre-tensioned concrete straps was compared to that of 50x25 mm steel straps. The tests proved that the concrete straps prior to cracking had twice the stiffness of that of the steel

straps; this clearly proved the viability of using the concrete strap to provide transverse confinement.

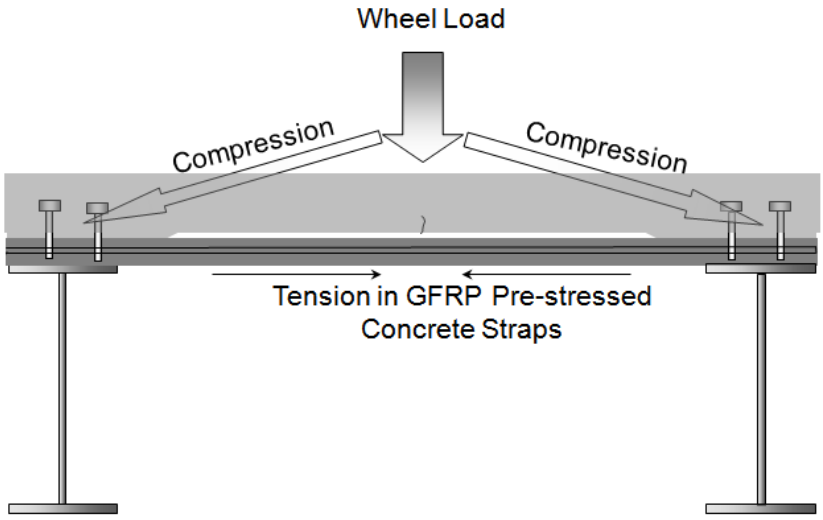

Figure 2.2 Steel-free bridge deck slab confined using GFRP prestressed concrete straps

Deck slabs designed using the empirical method, in accordance with the OHBDC/CHBDC, are expected to fail in fatigue. Slabs which fail in punching shear are those experiencing a monotonically increasing load, or static load and in the meantime the lateral restraint would not give in prior to the punching shear failure. So if it is assumed that the deck slab's failure load is at least 750 kN and it will only be subjected to a maximum wheel load of 207 kN, the deck slabs would not fail under fatigue in the lifetime of the structure.

Consequently, a steel-free deck slab, laterally confined with prestressed GFRP concrete straps, was tested to better understand the fatigue behaviour. The prototype bridge was a short span highway bridge framed longitudinally with composite steel girders. Two 9 m long girders were spaced 2 m apart and three prestressed concrete straps were placed one meter apart to confine a 175 mm thick deck slab with 50 mm haunches over the girders.

The investigation was performed on the deck slab at the load levels of 150 and 208 kN by means of a hydraulic actuator reacting against a steel loading frame, which was attached to the laboratory's structural floor. The study concluded that the prestressed concrete straps can be used to confine steel- free bridge deck slab laterally as it has sustained half a million cycles of maximum lifetime factored wheel load proving that its fatigue resistance is as good as that of other deck slabs.

2.2 Studies on Durability of GFRP

GFRP is a composite material that is susceptible to attach to alkalis. Researchers often study the durability of GFRP under harsh experimental environments that the GFRP might not face in the natural concrete environment. Results of experiments using early generations of GFRP might not be applicable to the new generations, as the manufacturing processes have improved to overcome the GFRP's vulnerability to environmental conditions. Reduction factors considered by design codes are conservative, since evaluating the durability of GFRP is difficult and has not been standardized yet. This section presents an overview of some of the many experimental techniques that have been applied to GFRP to define its long-term durability, while the conditions applied in the experiments will be categorized into weathering conditions with or without sustained loads. This section will also present some of the structures that used GFRP as reinforcing material successfully. The demonstration projects proved that GFRP is durable in a concrete environment; thus enhanced experimental procedures must be developed to reflect the long-term behaviour of GFRP.

Steel reinforcement faces corrosion problems, which require high maintenance and rehabilitation costs. These problems arise during winter, when fluctuation in temperature occurs and de-icing salts, the main catalyst of corrosion, are extensively used. The expansive corrosion property of steel can cause cracking and spalling within the concrete cover. The use of FRP as a reinforcement can overcome problems associated with the corrosion -prone nature of steel.

FRP is known for its high durability, great bond with concrete, resistance to harsh chemical environment, as well as its electric and magnetic neutrality. Glass FRP (GFRP) is cheaper than aramid and carbon FRP's, and the industry finds its use more attractive. However, its durability becomes the governing factor when performing a Life Cycle Cost Analysis (Benmokrane. & Cousin, 2005). Durability is the ability of the material to retain its physical and chemical properties over time (Bubani. et al., 2001). Much research has

been done on the durability of GFRP, but much more is in progress due to the various aspects of the material that still require exploration.

Glass fibres are protected by resin matrices. The matrix may degrade, however, due to its plasticization and swelling in the presence of water and other harmful agents. It is important to perform aging tests on GFRP to simulate real life scenarios by which the long term durability of GFRP can be assessed (Chen et al., 2006). According to available literature, contradictory conclusions have been given about the durability of GFRP, and its degradation mechanism in an alkaline concrete environment. The durability of GFRP was studied extensively in simulated accelerated tests where the GFRP reinforced concrete specimens used were highly porous and submerged in water of a high pH at elevated temperatures up to 80 ^{o}C (Memon & Mufti, 2004; Onofrei, 2005). Mechanical tests applied to these specimens suggested a reduction in the bond strength, shear strength and in Young's Modulus, (Sen, 2002; Bank et al., 1998). In one of the experiments, the specimens were submerged in pure sodium hydroxide, with the result that the researchers did not recommend GFRP as reinforcement for concrete (Uomoto, 2000). Contrary to previous accelerated aging tests, tests were performed on GFRP reinforced specimens exposed to an alkaline solution at a temperature of 20-38 ^{o}C for a 12-month period (Sheard, 1997; Onofrei, 2005). These researchers reached an overall conclusion that GFRP can be used as a reinforcing material in a concrete environment.

Although many experiments have been undertaken on the durability of GFRP reinforced concrete, there are several variables, such as environmental effects and sustained stress that have not been thoroughly investigated. It is for this reason that design guidelines account for conservative reduction factors (ISIS, Design Manual 3, 2001). In order to confirm the 50-75 year life cycle performance, critical test methods need to be established by which the durability of GFRP can be determined (Chen et al., 2006).

2.2.1 Accelerated tests for Evaluation of Long-term Behaviour of GFRP.

It is necessary to understand the various modes of degradation since the durability of the composite material is directly related not only to the strength of the constituent materials, but also to the integrity of the interface of the matrix and the fibres while aging. It was pointed out by Karbhari (2003) that the degradation of GFRP is mainly due to matrix related problems, such as the deterioration of the fibre/matrix interface. The weakening of the composite material is due to the deterioration of the interface between the matrix and the fibres, thus reducing the transfer ability of the loads between the fibres.

The analytical and experimental behaviour of GFRP can be classified into categories in which the first one is to evaluate the residual properties of composites after being exposed to a number of environmental conditions without loading, and the second category includes the effect of sustained loading (Nkurunziza, 2005).

2.2.1.1 Weathering Environment without Sustained Loading.

Chen, et al. (2006) applied their experiments on E glass fibres bonded with vinyl ester resin. Two types of GFRP were used (GFRP1 and GFRP2), produced by the same manufacturer. Both were helically wrapped and slightly sand coated. GFRP2 was the only one that was commercially available. The durability performance of GFRP bars in a concrete environment was tested by placing the bars in an alkaline solution to simulate concrete pore solution. Tensile strengths were recorded for the bars before and after immersion in the alkaline solution (NaOH, KOH, and $Ca(OH)_2$). The trend in tensile strength values was considered as an indication of the durability performance of the GFRP bars.

Two types of solutions were used; each had a different pH. A pH of 13.6 was intended to simulate the pore solution of Normal Concrete (NC), whereas a pH of 12.7 was used to simulate the pore solution of High Performance Concrete (HPC). In order to accelerate the attack of simulated environment on the specimens, high temperatures ranging from 20-60^{o}C were used. It is important to note that the temperatures applied were below the glass transition temperatures of the GFRP bars. The use of GFRP 1 was examined in the first solution, while GFRP 2 was tested in the second solution.

The results indicated a decrease in the tensile strength with increase in time of exposure to the simulated environment for both GFRP bars at all temperatures. They also indicated an increase in degradation as the temperature of the solutions increases. It was observed that the degradation was significant for both GFRP specimens, although the time exposure is much shorter than the expected service life of each bar. The speed of degradation may be due to the direct contact of the specimens with the alkaline solution

The HPC has a lower alkalinity than the NC. It is therefore considered a less aggressive environment for the GFRP bars. The results showed a different rate of degradation with different simulated pore solutions. Chen, et al. (2006) recommended using elevated temperatures to accelerate the rate of degradation of GFRP bars

Chu and Karbhari (2004) introduced the concept of the percentage of regain of the performance of GFRP samples, when reconditioned, through the process of dry out, after being immersed in de-ionized water solutions at different temperatures for the same time period and same conditions as that of the initial preconditioning. This principle is not applicable to civil structures that are constantly submerged in water.
The percentage of regain due to reconditioning is determined as:

$$\%\,\mathrm{Re}\,gain = \left[\frac{(\sigma_t)_{dry} - (\sigma_t)_{wet}}{\sigma_o - (\sigma_t)_{wet}}\right] \times 100 \qquad \textbf{Equation2.2}$$

Where σ_o is the unexposed strength, $(\sigma_t)_{wet}$ is the strength after immersion for the time (t) in de-ionized water solutions at given temperature in consideration, and $(\sigma_t)_{dry}$ is the strength of the same set of conditions but after reconditioning at 23 ^oC and 46% relative humidity for 28 days, which is equal to the same period of conditioning. This equation represents a ratio between the values of regain due to reconditioning to the loss in the composites strength due to conditioning. In the case of applying the same procedure to calculate the percent of regain to reconditioned samples immersed in alkaline solution, the results showed a substantial decrease in regain after reconditioning, and even in some cases no regain, which indicates irreversible damage.

There is a relative loss in the first five to ten weeks, due to the immersion of the samples in water, most of which is recovered on drying. The damage caused from the moisture uptake is matrix plasticization. At the initial stages of reconditioning there is a substantial regain of strength, but as both time and temperature of immersion increase, the level of regain becomes lower. This can be explained by considering the higher temperatures of immersion to be a mode of acceleration of the system's deterioration in time; therefore, the fibre-matrix interface and even the fibres themselves face a higher degree of irreversible deterioration (Chu et al., 2004). The degradation of the GFRP bars faced were losses in the tensile strength and elastic modulus, which cannot be regained, when placed in an alkaline solution (Nkurunziza *et al.* 2004). The moisture absorbed is seen to attack the GFRP with free hydroxide ions that degrade the silica structure. When the GFRP is exposed to the alkaline solution, it experiences an irreversible damage observed under a scanning electron microscope by surface degradation and pitting. The observation can be explained by Si-O bonds in presence of -OH, resulting in a surface loss as well as pitting at areas of contact with high pH solution, such as concrete pore water and $Ca(OH)_2$ salts. The presence of water at the fibre surface would produce free alkali hydroxide groups that degrade the silica structure of the fibres.

The results of these extensive studies on the effects of moisture and alkaline solutions indicate that several factors take part in the degradation of GFRP material when exposed to different environments. The dominant modes of failure can be summarized as the following: the rupture of fibres, the cracking of the matrix, the loss of bond at the interface, or any combination of the three (Chu et al., 2006; Nkurunziza et al., 2004). The process that would lead to these modes of failure is highly dependent on the type of resin matrix; thus moisture uptake occurs at various rates. Capillarity at the molecular level occurs wherever cracks are produced at the interface or between the resin and the fibre. With an increase in weight, plasticization, and loss of stiffness, the matrix modules would be reduced. The stress- corrosion cracks produced during loading start the moisture uptake process, which initiates deterioration of the composites (Nkurunziza et al., 2004). The effecting environmental factors must be accurately assessed to better anticipate the long-term behaviour of these materials.

Nkurunziza et al. (2004) suggested that the use of hydrophobic resins could reduce the rate of degradation mechanism of GFRP. In another experiment conducted by Chen et al. (2006) the composite's ability to absorb water was defined to result in changes in the internal stress states, which results in a decrease in the glass transition temperature (T_g). An important gauge to the physical property of the matrix is T_g, as it is the only indicator to the structure of the polymer, its mechanical properties and also an indicator of its thermal stability (Mufti et al., 2005). On the occurrence of short-term plasticization and long–term hydrolysis to the ester links of the composites due to moisture absorption, a high level of molecular mobility is induced resulting in a decrease in the glass transition temperature. On testing the GFRP specimens by immersion in de-ionized water solution at different temperatures, it was observed by the researchers that the highest values of the resulting T_g came after immersion for a period of 5-10 weeks, and then a decrease as the duration of immersion decreases. This observation was explained by the occurrence of two competing phenomena that cause a fluctuation of T_g. The first is the induction of a higher molecular mobility of the composites due to the plasticization and hydrolysis

processes, while the second phenomenon is due to the residual post-curing of the vinylester polymers resulting in an increase in T_g.

In case of immersion in an alkaline solution, there is no clear response of an initial post-curing response of the specimens, although its effect may be seen after a 20-week period, as an initial decrease in T_g is followed by short plateau, then a continuous decrease in T_g.

On the other hand, Mufti et al. (2002) argue that results from testing GFRP samples in an actual concrete environment are different from simulated accelerated or non- accelerated tests applied on GFRP samples in alkaline sample.

It was proposed by Kharbari (2003), to express the drop in strength of GFRP reinforcements by coefficients of reduction when facing short-term or long-term exposure. For a long-term exposure the coefficients used should vary between 0.25 -0.5, whereas the ISIS Manual 3 proposed a reduction coefficient of 0.4 for GFRP (Nkurunziza et al., 2004).

2.2.1.2 Weathering Environment with Sustained Loading.

According to Nkurunziza et al. (2004), the combined effect of load and environment have not been fully carried out to better anticipate the long-term performance of GFRP specimens exposed to different environments (water, alkaline and sea water) in the presence of loading at various temperatures. The applied stress levels were much larger than those applied under service conditions to accelerate the process. In the meantime elevated temperatures were also used as a degradation factor to the composite material. At low stress levels the visco-elastic behaviour of the constituent materials prevents the formation of cracks, thus preventing the passage of the deteriorating material to the matrix. Micro-cracks are formed in the matrix of GFRP bars, due to high stress levels that create a network of cracks that aid the penetration of a number of harmful agents to reach

the core of the bar. This indicates that at low stress levels there is a stress threshold that prevents the occurrence of micro-cracking, and the dominating factor of degradation is the capillarity flow.

AlMusallam et al. (2006) conducted a set of experiments on concrete beams reinforced with GFRP that were surrounded with high alkaline cementitious paste. The purpose of the alkaline paste is to help extraction with minimal damage, as well as to induce an alkaline environment for age acceleration. Three groups of beams were exposed to different environmental conditions in three separate tanks containing: tap water, seawater, and wet dry cycles with two weeks exposure to seawater. The experiments were conducted at a controlled temperature of 40^{o}C. Each tank contained twelve beams; six of them were not loaded while the remaining six beams were loaded with dead weight causing stress in the GFRP bars of 20-25% of their ultimate stress. Duration of the exposure to the different environmental conditions is an important criterion in defining the long-term behaviour of the GFRP bars. Four beams were removed (2 stressed and 2 unstressed) from each tank to be tested at 4, 8 and 16 months. Two test samples were made from each extracted bar to apply a tension test on them. It was observed the effects of the load were apparent after 16 months exposure. The specimens under sustained loads experienced:

- A 30% higher loss in strength than those unstressed in case of specimens immersed in tap water.
- A 28.92% higher loss in strength than those unstressed in case of specimens immersed in seawater.
- A 33.2% higher loss in strength than those unstressed in case of specimens experiencing wet/dry cycles.

This procedure shows no apparent difference among environmental conditions on the tensile strength of the GFRP bars under the same sustained load. Another set of beams was prepared to study the effect of both the environmental factors and sustained loading, for a duration of 8 months, on the load deflection behaviour of GFRP. When analyzing the load-deflection curves for the unstressed beams, it is apparent that a bar slippage occurs at low load levels, through the formation of sudden peaks and valleys. This

observation was not present in the stressed curves, probably due to its occurrence earlier during the initial loading of the dead loads at different environments. The specimens under sustained loads required:

- An 18.1% lower load level for failure than the unstressed in case of specimens immersed in tap water.
- A 1.1% lower load level for failure than the unstressed, in case of specimens immersed in seawater.
- A 12.5% lower load level for failure than the unstressed in case of specimens experiencing wet/dry cycles.

When lower loads were applied, the stiffness of all unstressed beams was the same at the initial stages, but as the applied loads increased, the stiffness of stressed beams was higher for all environmental exposure conditions. This behaviour can be explained by bar slippage. On the other hand both stressed and unstressed beams faced a reduction in ductility due to the presence of the sustained load and/or the environmental exposures.

Several experiments were conducted in a similar manner where Sen et al. (2002) provides evidence that when GFRP bars are under constant loading of 10% of their initial strength and immersed in an alkaline solution of pH 13.5, they could lose up to 70% of their tensile strength. On the other hand, Nkurunziza et al. (2005) tested GFRP bars that were immersed in alkaline solutions as well as de-ionized water solutions. The specimens were immersed in the solutions while being under the effect of sustained loadings of 30-40% of the ultimate strength. In order to accelerate the aging process the specimens were subjected, in the mean time, to different temperature levels between 55-75^{o}C for up to 60 days. A loss of only 4-11% was obtained when these bars were tested.

2.3 Demonstration Projects Present in North America, Using GFRP as a Reinforcing Material.

There are a number of bridges built with GFRP bars and grids for the purpose of crack control, in which the grids are placed in the top layer of concrete deck slab to delay the corrosion process of the main reinforcement. ISIS Canada studied the durability of five

GFRP in field demonstration structures by removing at least ten concrete cores containing the GFRP reinforcement from each demonstration structures.

During the construction of each of these bridges, control specimens were set aside in order to compare them with the cores removed from the structures after facing years of in situ conditions. The five structures chosen are located across Canada and face different environmental conditions, such as de-icing salts, sea water, splash and tidal, wet and dry cycles, as well as freeze and thaw cycles. These structures are: Hall's Harbour Wharf in Nova Scotia, the Joffre Bridge in Quebec, the Chatham Bridge in Ontario, the Crowchild Trail Bridgein Calgary and the Waterloo Creek Bridge in British Columbia. It is important to note that the GFRP reinforcements placed in the bridges were for crack control purposes, except for Crowchild Bridge, where the GFRP was placed as a main reinforcement. The purpose of the investigation was to understand the reality of the alkali attack on the GFRP in actual structures by comparing the in-service cores with the control specimens. Based on the results of several durability tests made on GFRP, the Canadian Highway Design Code (CHBDC) has limited its use to secondary reinforcement. The objective of the study done by Mufti et al. (2005) was to understand the reality of the performance of GFRP in the demonstration structures, experiencing actual service conditions, which is likely to be different than the results deduced from simulated tests (Mufti et al. 2005).

Micro-structural tests were used to identify the state of degradation of the GFRP materials as well as the condition of the alkalinity of the concrete. These tests are: Optical Microscopy (OM), Scanning Electron microscopy (SEM), Energy Dispersive X-Ray (EDX), Differential Scanning Calorimetry (DSC), and Fourier Transform Infrared Spectrometry (FTIS). The preparation procedure of the samples required great attention and care, since during the preparation the GFRP can get scratched, or the matrix and concrete may debond or can experience micro-cracking, or the polished surface of the matrix and concrete may get contaminated from one sample to the other.

The following summarizes the purpose of each of the micro-structural tests:

- OM focuses on the boundary between concrete and GFRP. With good bond between concrete and GFRP there is an effective mechanical load transfer system between the two materials. As the bond degrades at the interface, delamination occurs, and gaps form facilitating the accumulation of water and forming areas having different moisture content, alkalinity, thus accelerating the degradation process (Onofrei, 2005). The results of the examinations proved that there is a good adherence between the two materials.

- SEM is applied to address the soundness of the constituents, both fibre and resin, of the composite material. In case of deterioration of the interface of the fibres and the matrix, the gaps formed allow the access of aggressive substances to the glass, and so the glass dissolution process will take place. The results of the SEM showed there is no evidence of any gaps present and that the individual fibres were intact (Mufti et al. 2005).

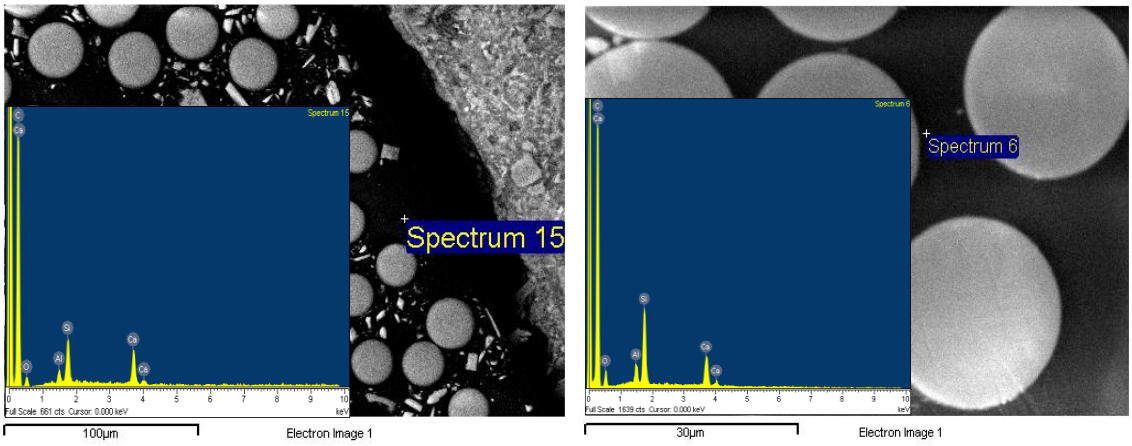

Figure 2.3 Comparing EDX images for Joffre Bridge for Structure's Sample (Left) and the Control Sample (Right) (Onofrei, 2005)

- EDX is used to analyze the chemical composition of the GFRP in the core samples and compare them to that of the control samples. The chemical composition and distribution in the GFRP fibres changes when starting to degrade, especially when the alkalis from the concrete pore solution find their way into the polymer matrix. The results from the

EDX example of GFRP specimens removed from the Joffre Bridge, as shown in Figure 2.3, are almost identical to those of the control specimen.

- DSC is used to detect the decrease in T_g of the GFRP of the core samples, in case of the presence of alkalis or water, as well as detecting if during the manufacturing process the GFRP materials used were sufficiently cured. This phenomenon is known as the cross-linking or post-curing process (Benmokrane, & Cousin, 2005). It was noted by Mufti et al. (2005) that the T_g values of the GFRP bars reveal no disruption of the resin/fibre matrix due to the exposure of the natural factors of deterioration, even in the case of Joffre's Bridge, which had a lower T_g than that of the GFRP used in other structures. The reason behind the decrease in the values was deemed to be due to the manufacturing process, since the other tests suggest no degradation in any of the GFRP constituents.

- FTIS is used to define whether disruption in the resin's chemical structure has occurred or not. Any disruption can consequently cause a change in the material properties of the GFRP constituents. The clue to any hydrolysis occurring to the matrix polymers would be the change in the amount of hydroxyl groups in the composite material. It is true that the chemical structure of the vinylester resin is composed mainly of hydro-carbon links and hydroxyl groups, but by comparing the spectrum of the site's samples to that of the control sample, the migration of hydroxyl ions can be detected (*ibid*). The results of the FTIS indicate no degradation occurring to the vinylester polymers, due to the similarity between the spectrums of both the core and the control samples (Mufti, et al. 2005).

The tests confirmed that no degradation of GFRP occurred when placed in the concrete environment and exposed to real service conditions, as seen in Figure 2.3. The Technical Subcommittee of Fibre Reinforced Structures of the CHBDC has, as a result of the study, approved the use of (CSA - S6-02, 2002) GFRP reinforcement as a main reinforcement and as prestressing tendons in concrete structures.

Benmokrane et al. (2004) presented a study on four bridges, three of which are in Quebec (Joffre Bridge, Wotton Bridge and Magog Bridge) all reinforced with both GFRP and CFRP, and one in the USA (Morristown Bridge) that is reinforced, top and bottom mesh,

with GFRP. These bridges are considered demonstration projects on the performance of GFRP as a reinforcing material, through field testing and remote monitoring (Benmokrane, et al. 2004).

Upon completion of construction, heavy trucks were used to calibrate the stress level in the reinforcement in the deck slab, when applying static and dynamic loading. The dynamic responses were documented using computer-aided data logging systems. The maximum tensile strain observed in the FRP reinforcement is 0.16 of the ultimate strain of the material, when under serviceability conditions. Remote structural health monitoring systems were attached beneath Joffre, Wotton and Magog Bridges to aid in predicting any possible degradation of the bridge, and to provide it with the proper maintenance. According to the variations in the recorded strains, it was obvious that the effect of temperature with time was the major factor influencing the fluctuation in strain. The temperatures ranged between -18 and 33^{o}C, where as the strains recorded in the FRP bars varied from -520 to +440 micro-strains, representing 3-4% of the ultimate strain leading to rupture of the material. Additional visual inspections were made to the remote monitoring to document any propagation of cracks on the top and bottom surfaces of the deck slabs. Based on these studies, the research team felt confident that these bridges reinforced with FRP provide competitive performances to those reinforced with steel, under serviceability conditions.

Chapter 3

Design of Prestressed Concrete Straps

3.1 General

The preliminary details of a concrete strap prestressed with GFRP, following the CHBDC Clause 16.7 guidelines discussed in section 2.1.4, are developed for an external deck slab panel on girders at a spacing of 2.0 m. The deck slab is 175 mm in thickness and the concrete is proposed to have 45 MPa strength and having a modulus of elasticity of 27900 MPa. Banthia (2003) has selected the straps' spacing to be 1.5 m and so the area of the strap could be computed using equation 3.1.

$$A = (F_s \times S^2 \times S_1 \times 10^9) / (E \times t)$$

$$= (6.0 \times 2^2 \times 1.5 \times 10^9) / (27900 \times 175)$$

$$= 7364\ mm^2$$

Equation 3.1

The connection of the strap to the supporting beam should be a minimum of 200*A*. The shear connecting mechanisms are placed on the beam in the vicinity of the straps which are within 200 mm of the nearest strap, and that is the basic requirement for steel straps. The straps made of FRP should be placed at spacing, such that it would give conservative results. It is worth noting that equation 3.1 would have led to A = 1029 mm^2 for straps made of steel, having a modulus of elasticity of 200,000 MPa. The connection strength, i.e. 200*A*, is calculated by using this area, as the use of concrete area in equation 3.1 would lead to unnecessary high connection strength. The connection strength for the concrete strap = 200 x 1029 = 205,800 N = 205.8 kN. In light of this equation, the

maximum tensile force that the concrete strap will ever experience is 205.8 kN. Newhook and Mufti, (1996) have measured strains in the straps of a full scale model of a steel-free deck slab for a wheel load of 400 kN which led to a tensile force of 50 kN in the strap, as previously explained in Section 2.1.4. The strap will be designed for a maximum tensile force of 100 kN, that is double the experimental tensile force. The load at which the strap fail would correspond to a combined wheel load of about 800 kN. That combined wheel load is nearly 2.8 times the factored design load for the ultimate limit state. Banthia (2003) has provided an external transverse confining system by means of concrete straps, which were kept from cracking by means of prestressing. The stressing was provided by means of GFRP bars. The properties of the GFRP bars of 14.9 mm in diameter are the following:

Ultimate tensile strength	= 886 MPa.
Modulus of elasticity	= 41.15 GPa.
Standard deviation of tensile strength	= 21.18 MPa.

The CHBDC (2000) permits a maximum jacking stress of 23% of the 5^{th} percentile tensile strength in GFRP tendons, or 467 MPa. The required area of cross-section of GFRP bars to sustain a tensile force of 100 kN, is 26 mm^2. The two #5 GFRP bars, each with a diameter of 14.9 mm, provide a total cross-sectional area of 349 mm^2. These bars, stressed at 377MPa, would provide a total tensile force of 132 kN, even after prestress losses would be well above the design value of 100 kN. The cover of the concrete followed the CAN CSA S6 requiring 40 mm as a cover, resulting in a strap size of 100x150 mm with two 15 mm GFRP bars. Banthia (2003) prestressed the bars at 45% of its ultimate strength and tested, proving that it is a viable structural element to be used in the steel-free bridge deck slab and having more than twice the stiffness of conventionally used steel straps 50x25 mm in cross section.

3.2 Design Size of the Strap

Hoyer's effect is the radial and circumferential pressure induced at the release of prestressing that may cause the development of a longitudinal crack in the straps (Leonhardt, 1964, de Scutter, Matthys, & Taerwe, 1997). As it is part of the research program to prestress three straps to 55% of the ultimate strength of the GFRP, the Hoyer effect became an issue that needed to be considered. The Hoyer effect was calculated and will be discussed at a later section. The strap size was increased to 160x 100 mm in addition to placing spiral reinforcement around each bar at the transfer zone to prevent the concrete from instigating a splitting failure of the straps. Figure 3.1 presents the cross section of the samples tested in this experimental program.

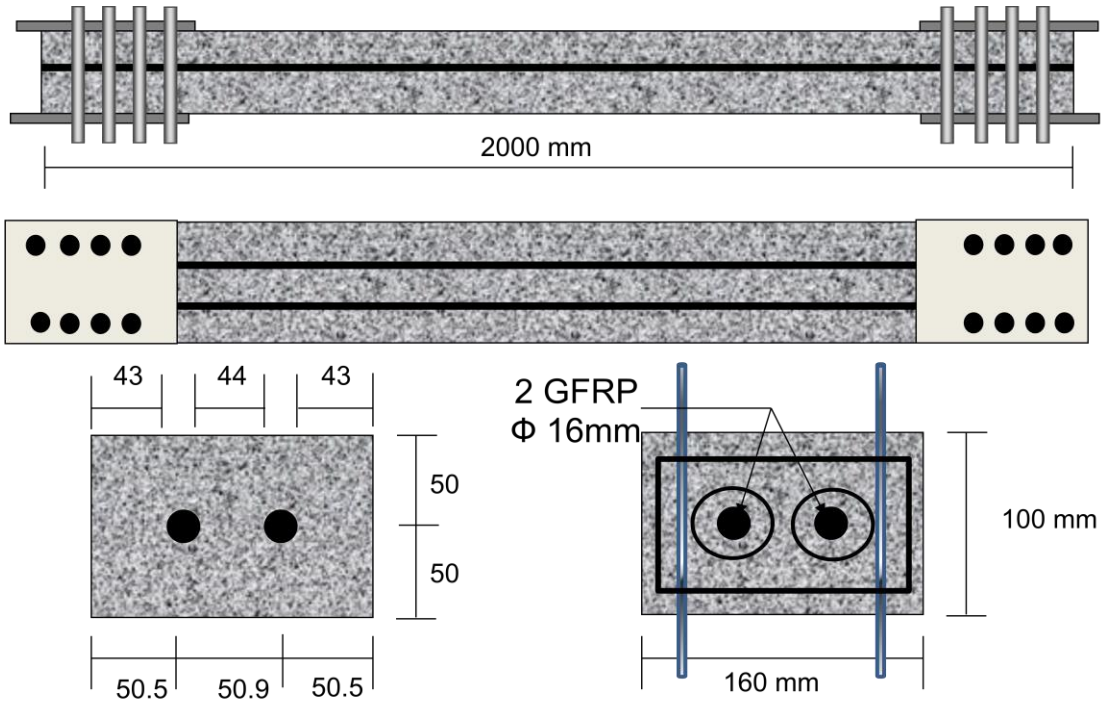

Figure 3.2 Detailing of the GFRP prestressed concrete straps.

Due to the unavailability of the 14.8 mm diameter GFRP bars, this research was conducted using the 16 mm diameter C-bars manufactured by Pultrall. The properties for the #5 V-ROD needed for the design process were available through the manufacturer and quoted as follows:

E_f	= 46 GPa
f_u	= 794 MPa
E_{ff}	= 1.8%
v	= 0.26

Leonhardt (1964) described the Hoyer effect as the swelling of the tendon that occurs during the release of the tendon from its temporary anchorage. The GFRP bars are to be prestressed up to 55% of their ultimate strength, and the Hoyer effect was a concern that needed to be addressed due to potential cracking at release as seen in Figure 3.2. De Shutter et al. (1997) also described the Hoyer effect for FRP materials as a wedge-shaped expansion of the prestressing element in the anchorage zone. The swelling of the tendon produced radial pressure on the concrete wich may be quite significant depending on the level of prestress. This radial pressure consequently produces tension in the circumferential directions which causes the splitting cracks.

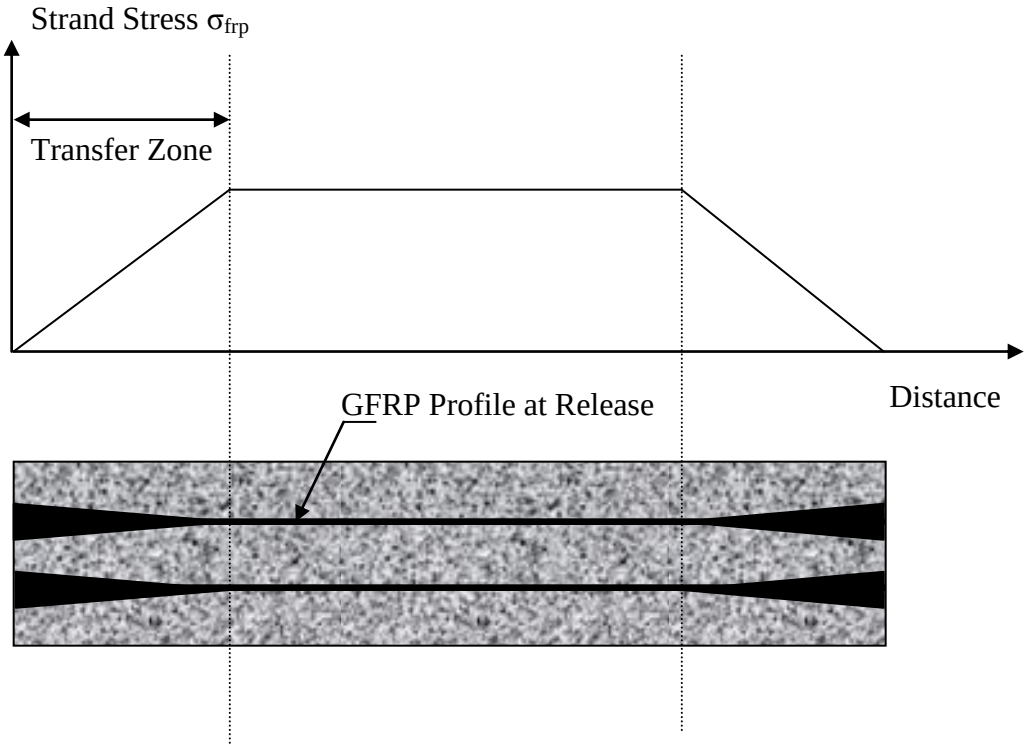

Figure 3.2 Hoyer Effect causing the Lateral Expansion of the GFRP at Transfer Zone.

The circumferential stress due to the Hoyer effect can cause splitting cracks if the concrete does not have the required tensile strength to overcome the splitting forces. The circumferential stresses need to be calculated to find out the required tensile strength for the considered prestressing level. The calculations were performed according to Davoudi (2009).

Using the values of the material properties of GFRP published by Vogel (2005), the stresses induced during the prestress release were calculated and presented in Figure 3.3. It can be observed that there is a high radial stress released from the bars onto the

concrete which exceeds its tensile strength, and since the bars are close to each other, there is a cumulative effect of the radial stress occurring between bars.

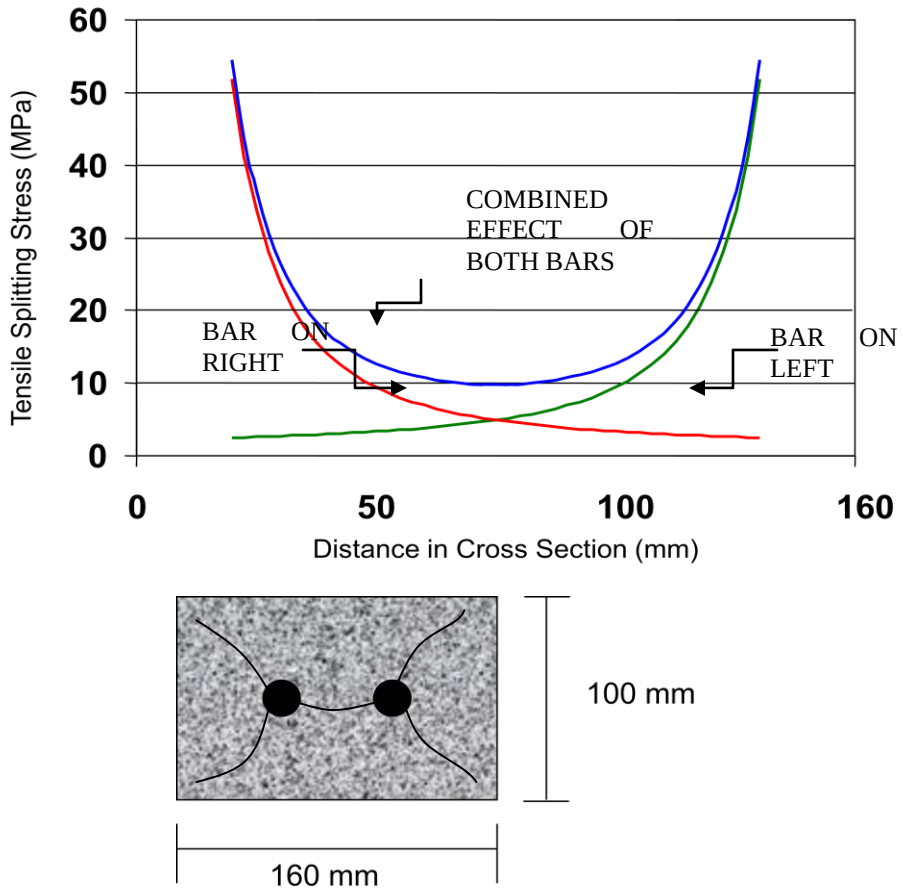

Figure 3.3 Model representing FRP cbar embedded in concrete.

It is necessary that the straps do not crack at prestress release and at service load levels, therefore, the concrete strength selected was 45MPa. The calculations concluded that it is imperative to place additional reinforcement at the anchorage zones of the straps to prevent splitting at release of prestress. In the detailing of the reinforcement it is important to shape the reinforcement to be able to be wrapped around the GFRP bars as the circumferential stresses are high and exceed the tensile strength of concrete between

the bars. After a careful study it was decided to use a spiral shaped wire with a diameter of 2.5 mm which was placed to provide the proper confinement. The wire was bent in the lab into a coil having a pitch of 20 mm. In addition to the coils a steel cage using 51 *x* 51 mm wire mesh was used and was bent to cover the transfer length of 375 mm at each side of the strap (Fig. 3.4).

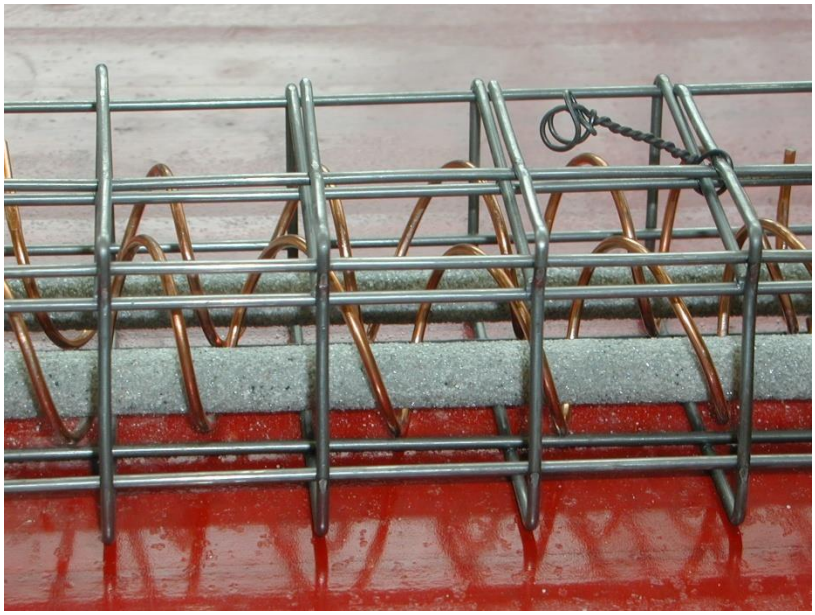

Figure 3.4 Reinforcing Cage Placed at the Transfer Region.

3.3 Casting of the Straps

Two #5 GFRP bars, with a trade name of V-ROD, and nominal diameter 15.88 mm were used in the two sample straps constructed in the lab. A resin sleeve type anchor using a steel pipe and expansive grout was used in this study. The geometrical dimensions for

sleeves were designed, following Annex B S806-02 (2002). The inner diameter of the anchor is 27 mm with 3 mm thick walls and the length of 450 mm.

Figure 3.5 Anchors Casting.

The anchors were thoroughly cleaned using a wire brush, soap and water, and left to dry to provide sufficient bond with the grout. The anchors were cast in a vertical position. Washers were glued to the ends of the sleeves to help in aligning the GFRP bars in the center of the sleeve. A wooden jig was designed to hold the anchors and bars specimens axially aligned. The wooden jigs, as well as the sleeves, were leveled to avoid any eccentricities in the bar during the curing time of the grout. The sleeves were filled with BRISTAR grout, which is a cementitious, highly expansive grout. The grout was mixed according to the manufacturer's instruction. The sleeves were then allowed to cure for 24 hours as recommended in the Annex B S806-02 (2002).

3.3.1 Design of Steel Couplers

Figure 3.6 Couplers for Prestressing of the GFRP bars.

The prestressing of the GFRP bars could not be completed using ordinary steel stressing chucks due to fear of the crushing of the bar at the grip causing the failure of the bars. Couplers were designed to adequately prestress.

the bars without causing any stress concentration at the anchor location. In this research it has been decided to prestress both bars using the same coupler to assure that both bars would be prestressed equally and when the prestressing is released there would be equal forces in the bars for symmetry.

The couplers were designed to ensure sufficient strength during the application of prestressing and were made using 300W steel of 20 mm in thickness; each coupler consists of two longitudinal steel plates welded to transverse plates at both ends. At the first end it is fitted with two holes for the anchors of the two GFRP bars each having a

diameter of 45 mm. The second end has a hole allowing the placement of a 30 mm diameter dywidag bar gripped with a chuck (Fig 3.6). Spacers were required and fabricated to prevent the anchor from sliding out of the hole during the application of prestressing.

The method of releasing was not the conventional cutting of the steel strand, but by unbolting the steel strand holding the steel bar to the abutment and then slowly releasing the prestressing to provide gradual transfer of the prestressing force to the structural element. This method ensures that the force released will be transmitted gradually and equally to both bars.

3.3.2 Instrumentation of the GFRP Bars

The GFRP bars were instrumented using 6 mm strain gauges in the longitudinal direction. These strain gauges helped in monitoring the strain during stressing process as well as the prestress losses during the concrete curing period. The strain gauges were placed at locations that would account for the elongation of the GFRP such that its final position after prestressing would be at third of each bar. Therefore, each strap was monitored using six strain gauges, three of which are on each bar at 500 mm intervals as seen in Figure 3.7. The strain gauges were connected to a monitoring box and provided readings during and after prestressing. These strain gauges helped in evaluating the ultimate strength and the modulus of elasticity of the GFRP bars.

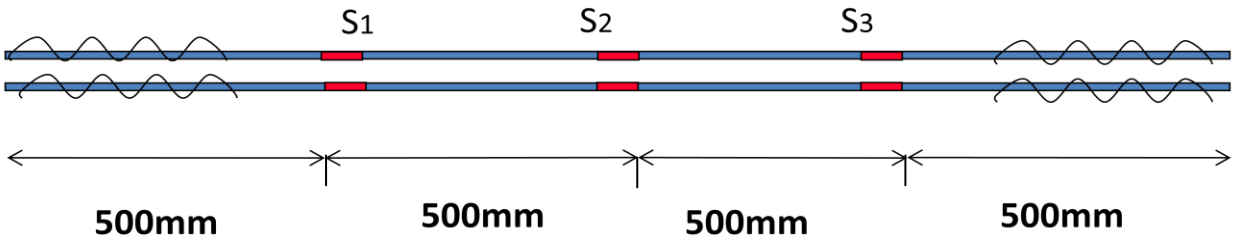

Figure 3.7 Strain Gauge Locations

3.3.3 Prestressing Setup

Prestressing and casting of the concrete straps took place at the University of Manitoba McQuade Structures Laboratory. The prestressing force was applied to the strands through the use of a hydraulic jack that was calibrated using a 267 kN testing machine to convert pressure readings into load (Fig 3.8 and 3.8b). Two specimens were cast in series in the same bed between the same bulkheads. The sides and bottom of the formwork were assembled around the strands prior to prestressing. The GFRP bars were centered with the help of the ends of the formwork, which were made of timber and had holes in them at the required height and width. The formwork ends were sufficient to hold the bars in place and avoid the use of plastic chairs which may contribute to crack initiation at their location.

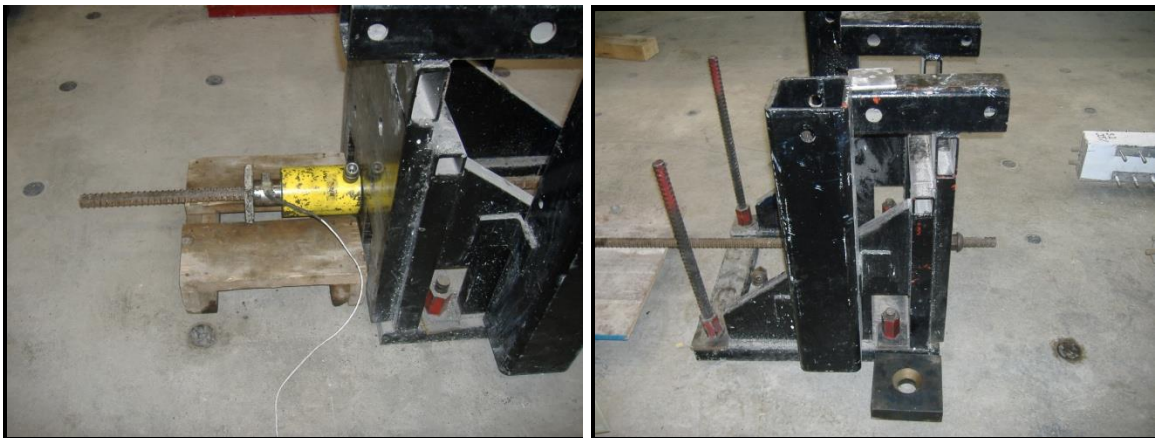

Figure 3.8 Prestressing Setup

Figure 3.8a Jacking End. **Figure 3.8b Dead End.**

The dywidag bars were then connected to the bulkhead that transfers the force from the prestressing to the 1m thick structural floor of the laboratory. The mechanism was conceptually similar to that used in the previous research of Banthia (2003). Figure 3.9 presents the prestressing set up for two straps.

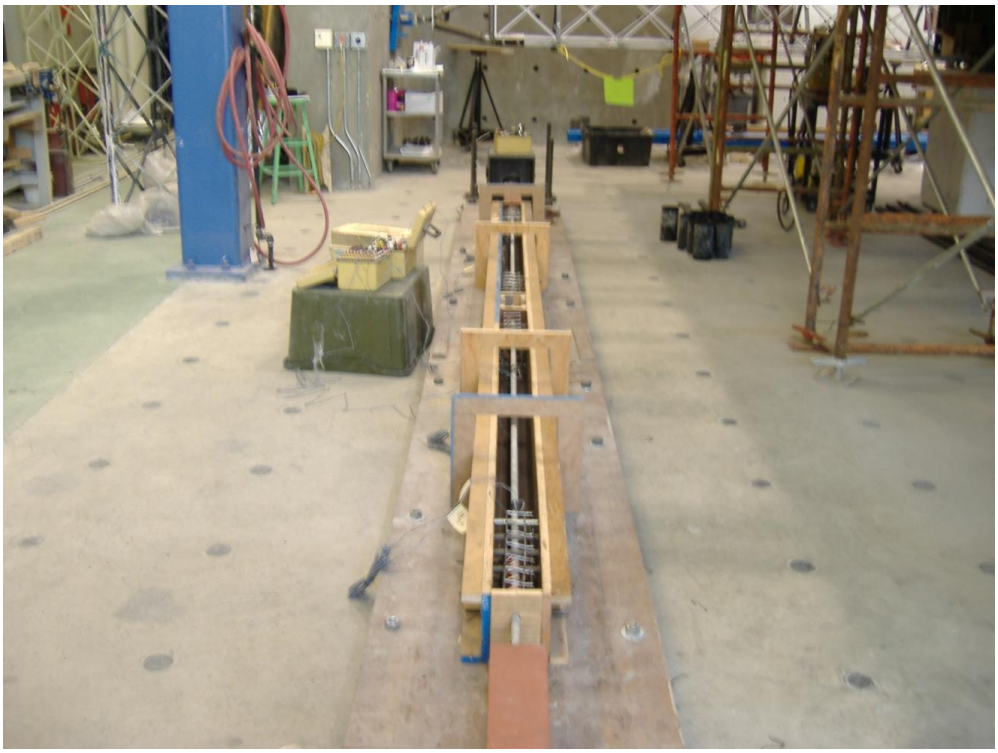

Figure 3.9 Prestressing Layout of the Straps.

3.4 Concrete

For the construction of the prestressed straps, 28 day strength of 45 MPa concrete was specified. The mixer used had a capacity of 0.085 m^3, which produced enough concrete for the two straps. Coarse aggregate with maximum aggregate design of 10 mm was used to satisfy the minimum clear spacing between the steel cages placed at the transfer zone. The mix design and the mechanical properties of the concrete used in the straps are given in Table 3.1.

Table 3.1 Concrete Mix Design and Properties

COMPONENT	VALUE
Type 30 Cement	500 kg/m3
Water	200 kg/m3
Coarse Aggregate	1034 kg/m3
Fine Aggregate	620 kg/m3
Slump	95 mm
Density	2417 kg/m3
Compressive strength	40.76 MPa
Elastic modulus	28787 MPa

Compressive strength and the splitting tensile force of the concrete mix were determined using the standard test for compressive strength, according to ASTM C 39 and ASTM C496/C 496M – 04. The tensile splitting strength is the governing factor in deciding when to release the prestressing force. It indicates the concrete's ability to withstand the tensile stresses transferred from the GFRP to the concrete at transfer of prestress. These tests were done before the release of the prestressing force, after 12 days and before testing the straps in axial tension. The results of these tests are presented in Table 3.2.

Table 3.2 Mechanical Properties of Concrete

No. of Days after casting	Compressive Strength MPa	Tensile Splitting Strength MPa
14	40.4	3.8
28	47.5	4
125	50	4.1

Figure 3.10 Testing for Mechanical Properties of Concrete

3.5 Prestressing of the Straps

Strains were monitored from the moment the GFRP bars were stressed, during release, and after release to monitor the prestress losses occurring in the straps. This was achieved by connecting the center strain gauges in the bottom and top bars of both straps to a strain indicator. The calibrated hydraulic jack was also attached to a load indicator box that allowed the verification of the prestressing load. Once the strain gauge readings, load and expected elongation were reached, the prestressing was locked by means of tying a nut against the abutment.

Prestressing was sustained for a total of 18 days, until the concrete compressive strength and splitting tensile strength were reached. The release of the prestressing was gradual by unlocking the nut slowly and preventing any cracking of the concrete. Strains were recorded before and after release of prestressing to confirm the estimated losses. Figure 3.12 presents the variation of strain with time after prestressing, and presenting loss of prestressing force due to relaxation as well as elastic shortening of the section at the time of release.

It was observed that the wooden formworks were not as stiff as was required; therefore the concrete ends were a centimeter wider than expected and did not fit the pulling mechanism. A circular grinder was used to grind that extra concrete until it fit the steel couplers of the pulling mechanism. The wooden formworks were damaged once removed and were deemed not re-usable. For the sake of productivity and for mass production, it was decided to design a steel channel section for six straps as they would be stiffer and reusable.

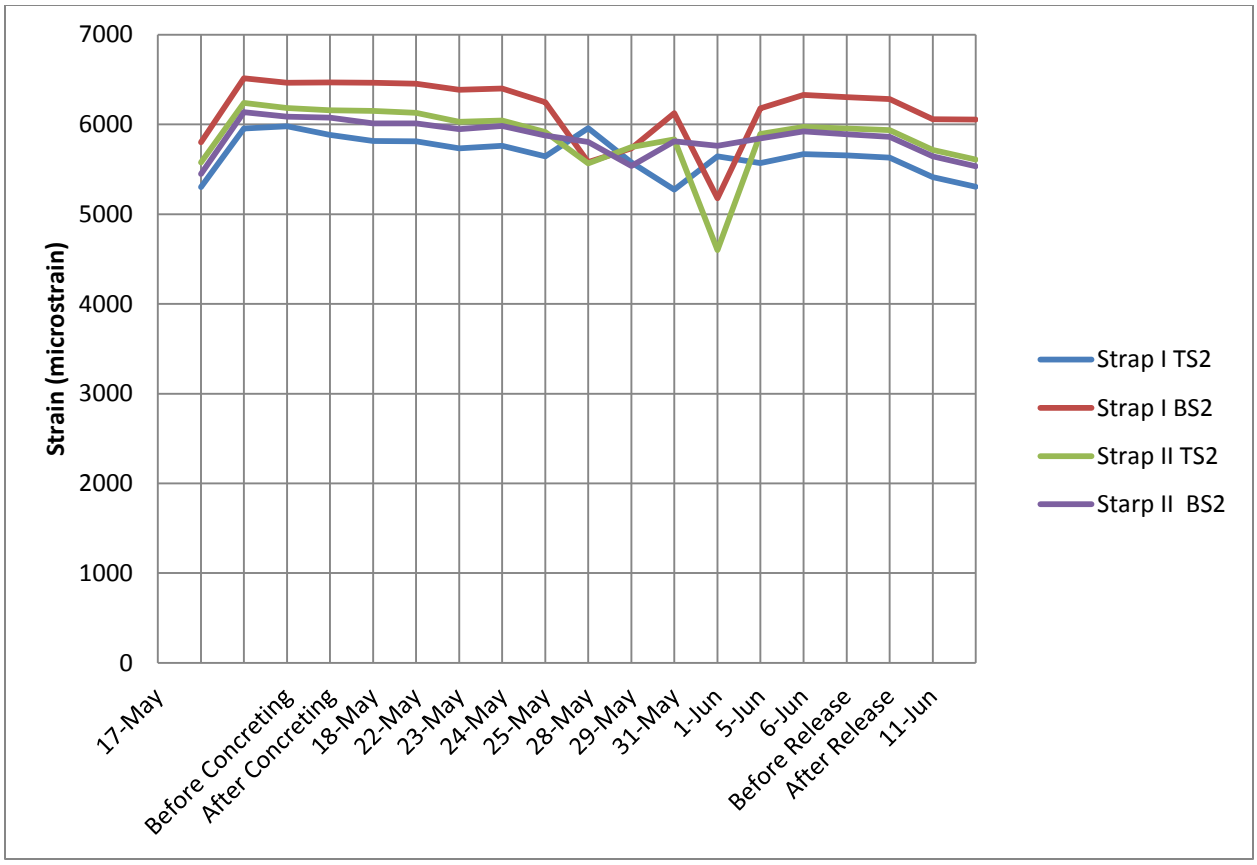

Figure 3.11 GFRP Strain Variation with Time

On the basis of the readings from Figure 3.11, a total prestress loss of 8.6% was estimated for the GFRP tendons after release.

3.6Testing Procedure

Each end of the strap has 8 threaded stainless steel rods placed in two rows before casting, which will aid the testing mechanism to grip the strap. Two 25 mm thick steel plates are placed at the end of the strap through the steel rods, as shown in Fig. 3.12. The length of the anchor is 350 mm. The steel plates are connected with a 32 mm dywidag bar using a steel coupler against the bulkheads, thus applying axial tensile force along the center of the strap.

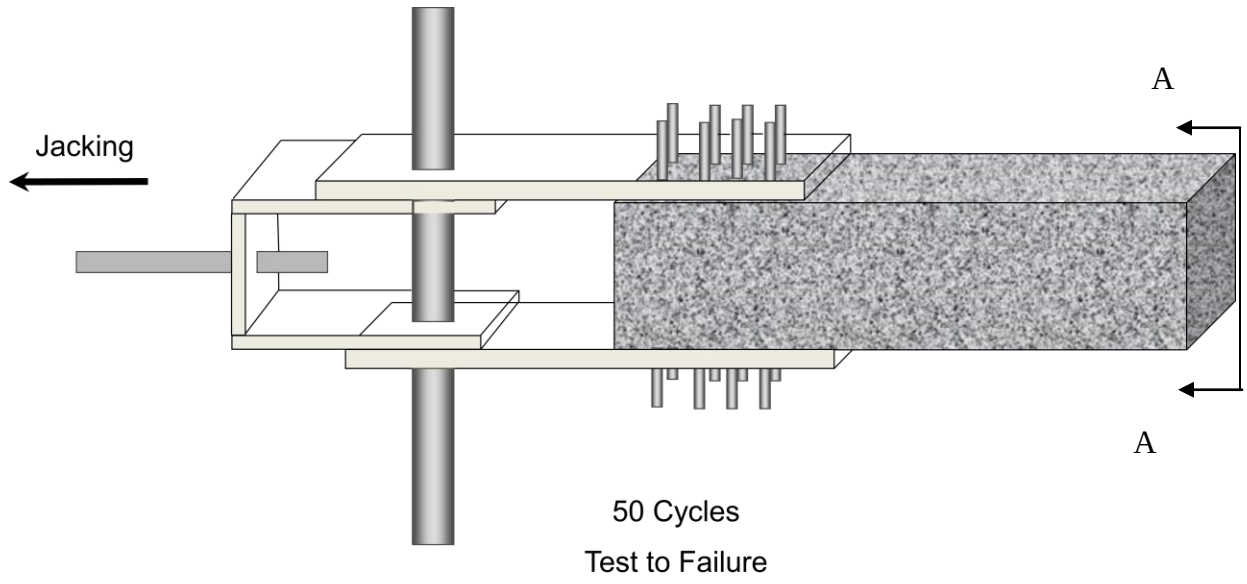

Table 3.12 Anchorage Zone Testing Mechanism

The straps were instrumented with a LVDT that spaned between the two anchors to measure elongation and five PI gauges to measure the crack width all placed on the top of the strap as seen in Fig. 3.13 and 3.14. In all the tests, the load was applied using a hydraulic jack that had the capacity of 70 MPa. The load was monitored with the help of a load cell. Both the load cell and hydraulic jack were calibrated prior to testing. All instruments were connected to a data acquisition system (DAQ).

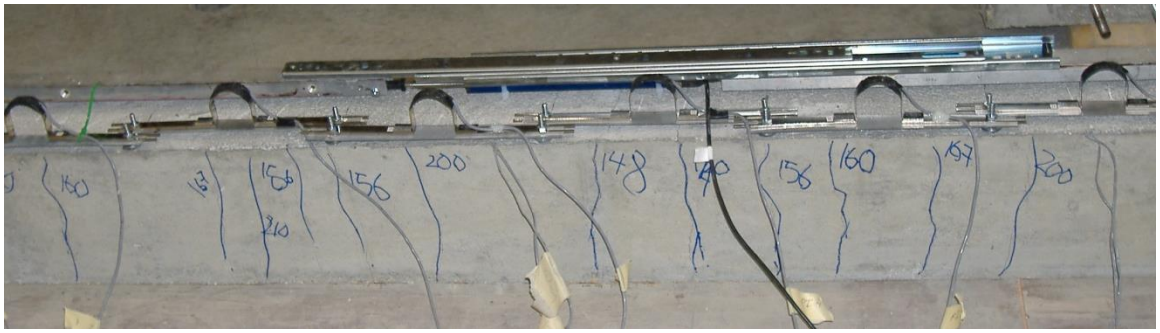

Figure 3.13 Instrumentation Placed on Straps

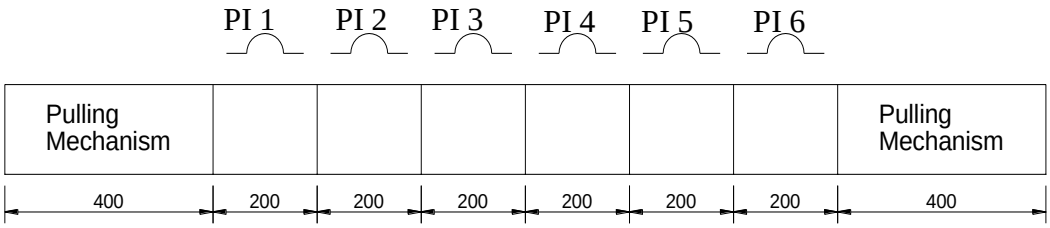

Figure 3.14 PI Gauges Diagram

Each strap was subjected to a fatigue test of 50 cycles of 50 kN load. The straps were then tested to failure. Initially, the samples were placed on the pres-stressing bed which was elevated from the structural floor to keep the straps leveled and assure that the load was applied at the center, thus preventing the development of any moment which would not occur in an actual strap in a steel-free bridge deck slab. During the cyclic loading the straps did not experience any cracking. When loading to failure the cracking pattern was observed at each load step and recorded until reaching the ultimate load. A typical cracking pattern is shown in Figure 3.15. The explosive and sudden rupture of the GFRP bars occurred at the center of the straps and is shown for Strap I trial 35% in Fig. 3.16.

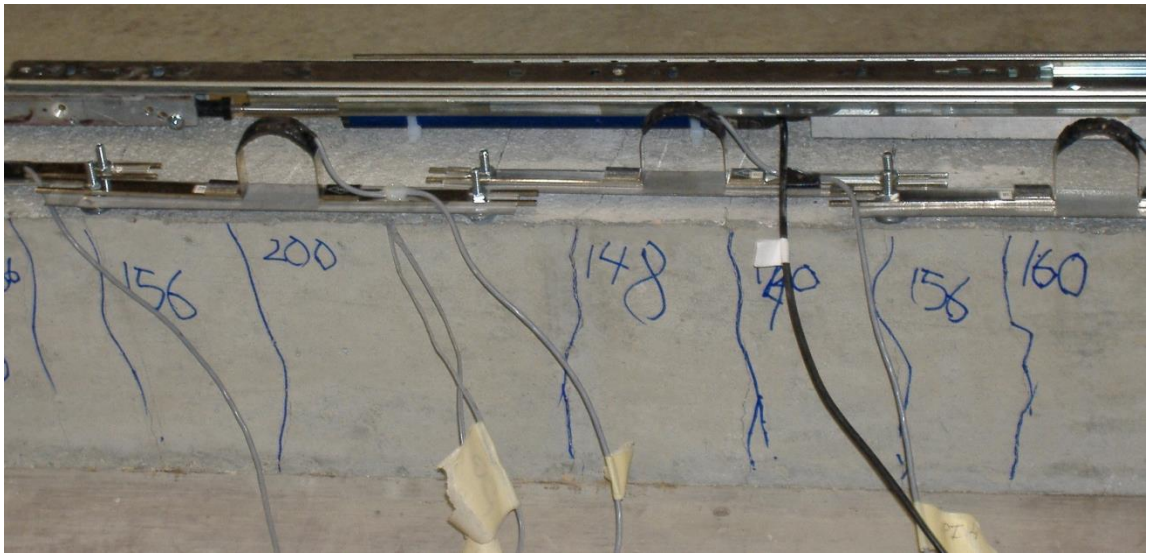

Figure 3.15 Cracking Pattern and Crack Spacing

Figure 3.16 Failure of GFRP Prestressed Concrete Strap

The trial tests did not show any problems with the samples and/or set-up, therefore the program continued as planned.

Chapter 4

Experimental Program

4.1 Introduction

An experimental program was undertaken to examine the behaviour of concrete prestressed with GFRP bars subjected to axial tensile forces. Nine straps were cast and tested, three straps at each prestressing level: 35%, 45% and 55%, and another six straps prestressed at 35% and 45% were cast and tested two and a half years later to assess their durability. Of each group of three straps, two straps were placed in the environmental chamber where they were subjected to fluctuating temperatures ranging between -25^{o}C to 45^{o}C. These straps were then tested and compared to the control strap left at room temperature. Each group of straps for each prestressing level was cast in series, released at the same time and using the same concrete mix. Hence, when the test results are compared, the only variable would be the temperature that the straps were subjected to.

4.2 Materials

4.2.1 Casting of Anchors for the GFRP Bars

The bars supplied by the manufacturer came in lengths of 10 m. The bars were cut using an electric circular saw for a length of 8.5 m which was long enough to cast the three concrete straps at a time. The strain gauges were placed on the GFRP bar before casting the sleeves in such a way that, after prestressing, the strain gauges would be in the desired

location; one at the center of the strap and others symmetrically at 500 mm from the center. A total of 12 strain gauges were placed on each bar. The bars were too long to cast the sleeves upright, therefore it was decided to cast them bent between two structural columns. The diameter of the bend was about 4 m, and a suitable wooden jig was placed to maintain axial alignment of the GFRP bars with the steel sleeves. The sleeves were designed in accordance with Annex B of CSA S806 (2002) as previously explained in Chapter 3. The setup of casting the anchors is shown in Figures 4.1 and 4.2. Thermo-coupler were placed at the center of the two bars of each strap to attain the actual temperature at the center of each strap when placed in the environmental chamber and compared to the temperature of the air circulating in the chamber.

Figure 4.1 Wooden Jig Alligning the GFRP Bar in Steel Anchor Sleeves.

Figure 4.2 GFRP Bars Bent for Casting ofAnchorage.

4.2.2 Prestressing Setup

A new prestressing bed was set up to accommodate the manufacturing of six straps at a time. The bed was 10 m in length and 1 m in width. One lineup prestressed the straps for 35% and the second line prestressed the straps at 45% for the first cast. The second cast was to prestress the straps at 55%. The third cast was for the straps designated for future research. Steel formworks were designed and manufactured using channel sections, C 150x12 mm, they were 2 m in length and had holes drilled at the required height and width for the stainless steel rods to go through as these are needed for the pulling mechanism. The anchorage zone is reinforced using the bent wire mesh cage as well as the stainless steel coils along the development length. To align the GFRP bars, wooden ends were used instead of plastic chairs to prevent the instigation of cracks in the concrete. The setup is presented in Figure 4.3.

Figure 4.3 PreStressing Setup

Before prestressing the bars, pre-mixed concrete was ordered following the specifications presented in Chapter 3, and it was to arrive three hours after the prestressing to allow some relaxation of the bars and at the same time not to allow the bars sit in the set-up stressed at high stress level without protection of the concrete. The sleeves of the bars for each lineup were connected to the coupler which was connected via steel tendons. The prestressing of the bars was monitored using a calibrated pressure gauge, strain gauges and verified mechanically by measuring the elongation during the tensioning process using a tape measure. The two bars of each lineup were stressed one at a time. After pre-tensioning, the bars were left to relax for several hours while the formworks were covered to safeguard against the explosive release of energy stored in these bars, since FRP tendons are brittle.

The prestressing for the 35% and 45% of the ultimate strength went smoothly. The stressing of the 55% straps experienced problems were the GFRP bars ruptured after stressing in one line-up (Fig. 4.4). The second lineup maintained the prestressing during casting, but ruptured after 12 days of casting and before release at the anchors and between the formworks. (Fig. 4.5). Creep rupture of GFRP was suspected to be the cause of these failures.

Figure 4.4 Rupture of GFRP After Prestressing

Figure 4.5 Rupture of GFRP After Casting

Two straps of those prestressed at 35% and 45% were placed in the environmental chamber to monitor their behavior and compare that with the behavior of the control samples. The straps prestressed at 55% were not placed in the environmental chamber, but tested in tension to observe their failure.

When discussing test results in the following sections, beams will be referenced by their names. These names differentiate the prestressing levels of 35%, 45% and 55%. The second part of the name identifies the location in the prestressing bed, where I represents the straps next to the dead end, II represents the straps in the center, and III represents the straps next to the jacking end. Straps prestressed at 35% and 45% with the connotation of I were the control samples and the rest were placed in the environmental chamber for durability study. The third part of the name A and B represents the sets pre- stressed and tested after 3 months of casting and those tested after 2 years of casting, respectively. The second set of straps were cast and left in the lab for two and a half years before getting tested in the same manner as previously discussed.

4.2.3 Prestressing Losses

Strains in the bars were monitored at various locations daily using a portable strain gauge monitor. The prestressing losses included long-term losses for the straps prestressed at 35% which ranged between 10% and 20% while the straps prestressed at 45% faced losses ranging between 15% and 25%. As for the straps prestressed at 55%, many of the strain gauges were damaged after the rupture and the readings indicated losses ranging between 15% and 45%.

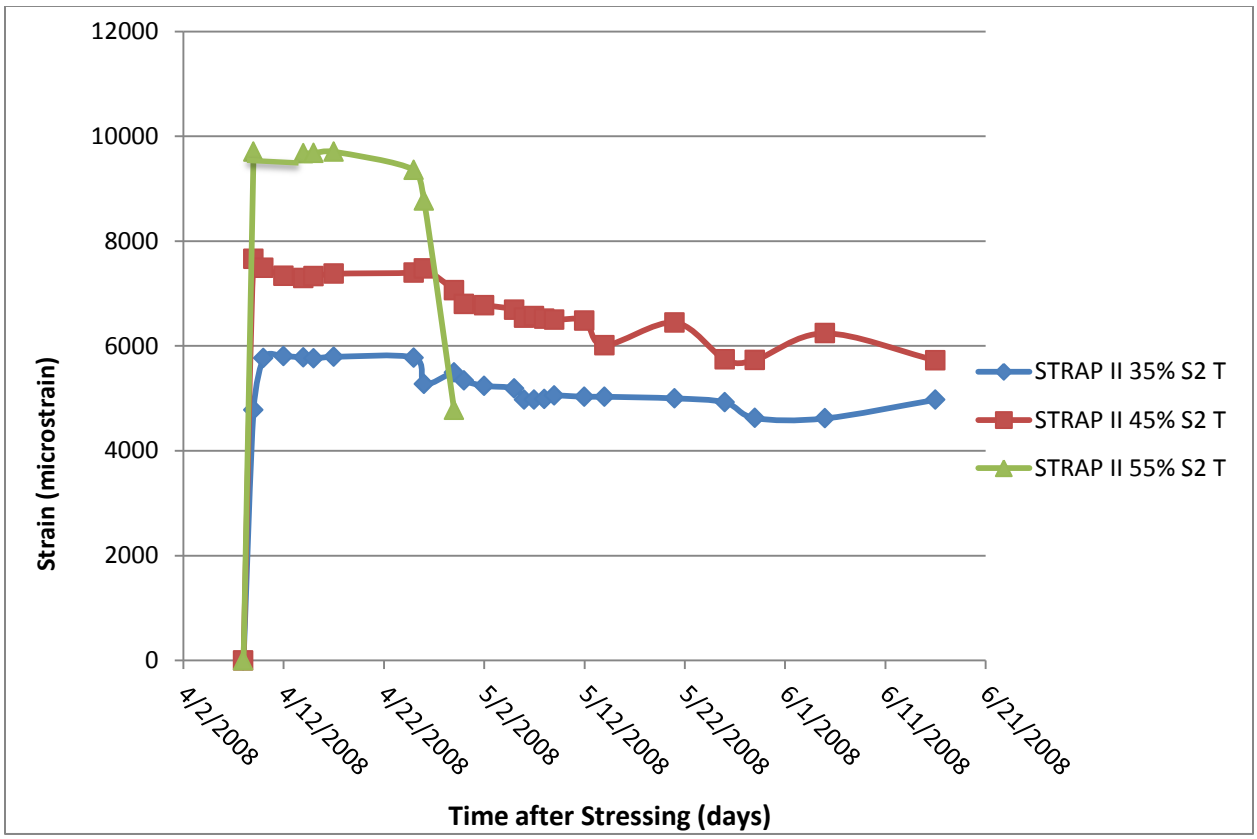

Figure 4.6 Prestressing Losses Observed

Figure 4.6 presents the losses of strain readings, of set A, monitored during casting and after release. This figure presents the losses occurring on the top bar of the middle strap in each line-up at different prestressing levels. To ensure the reliability of the strain readings at the time of release, prestressing losses were also estimated with Demec points

placed on the surface of the beams at the centre of the top surface of the straps of set B. Ten Demec points were placed at 20 cm intervals, which were then cemented to the straps using 5-minute epoxy after removal of the formworks. Figure 4.7 illustrates the prestress losses of the strap prestressed at 35% of the ultimate strength, which is consistent with readings from the strain gauges, as both strain reading methods show a loss of 400 – 500 μstrain within 25days, while Figure 4.8 presents that of the strap prestressed at 45% of the ultimate strength.

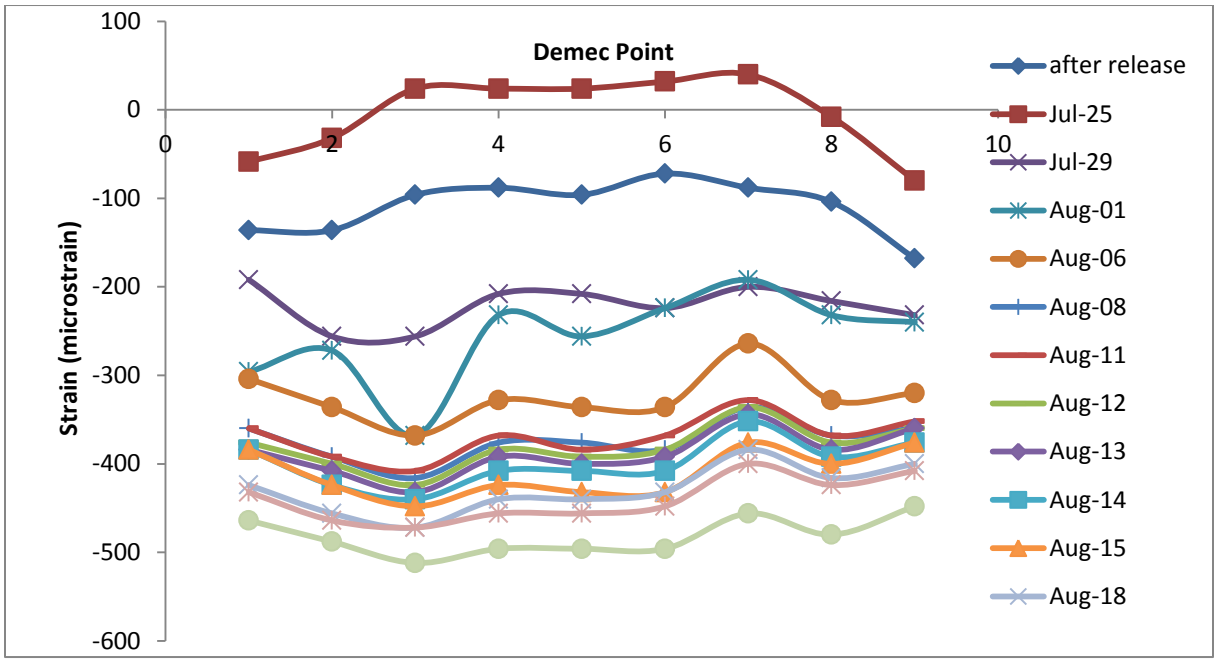

Figure 4.7 Prestressing Losses of Strap 35% I using Demec Points Readings

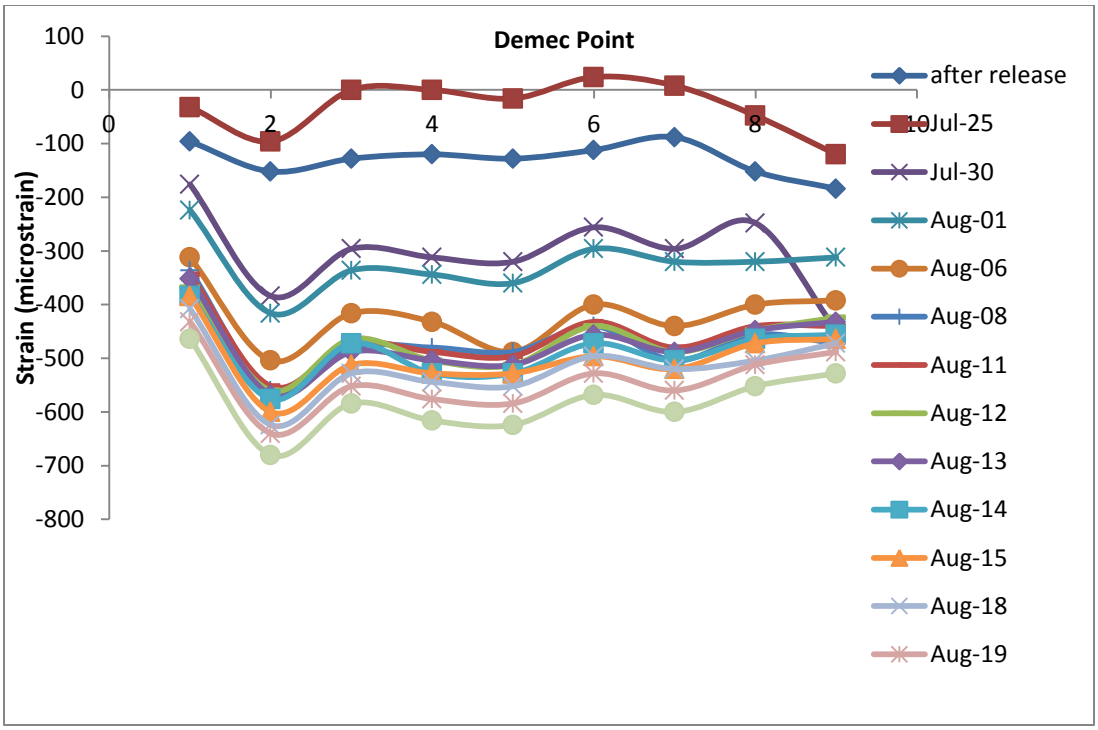

Figure 4.8 Prestressing Losses of Strap 45% I using Demec Points Readings

4.3 Durability Study

To evaluate the bond performance of prestressed GFRP bars in concrete environment under the effects of service temperature expected in the Canadian climate, it was initially decided to subject the straps to temperature cycles ranging between +40 ^{o}C and -40 ^{o}C. In the absence of standardized methods for durability evaluation, it was decided to follow the freeze thaw cycles from the studies performed at the University of Manitoba and developed by Mufti and Onofrei (2004), using ASTM E 1512 (1993).

The experimental program for the GFRP prestressed concrete straps is to expose the specimens to freeze-thaw cycles between -23 ^{o}C and 40 ^{o}C and a humidity of around 80% for 75 cycles. The straps that were tested two and a half years later after casting were exposed to the same conditions, but for 50 cycles only. Thermal cycling was

performed using an environmental chamber capable of reaching the specified temperatures with humidity control. The straps were then placed in the chamber at room temperature and placed on wooden blocks to prevent damaging the floor under excessive bearing stresses. Figure 4.9 presents the layout of the beams in the environmental chamber. This arrangement allowed for efficient air circulation around the samples to reach the desired temperature at the center of all the straps. Figure 4.10 shows the fluctuation of temperature in the environmental chamber with time, and Figure 4.11 indicates the variation of temperature at the center of the straps when conditioned to a Manitoba climate.

Figure 4.9 Arrangement of the Straps in the Environmental Chamber

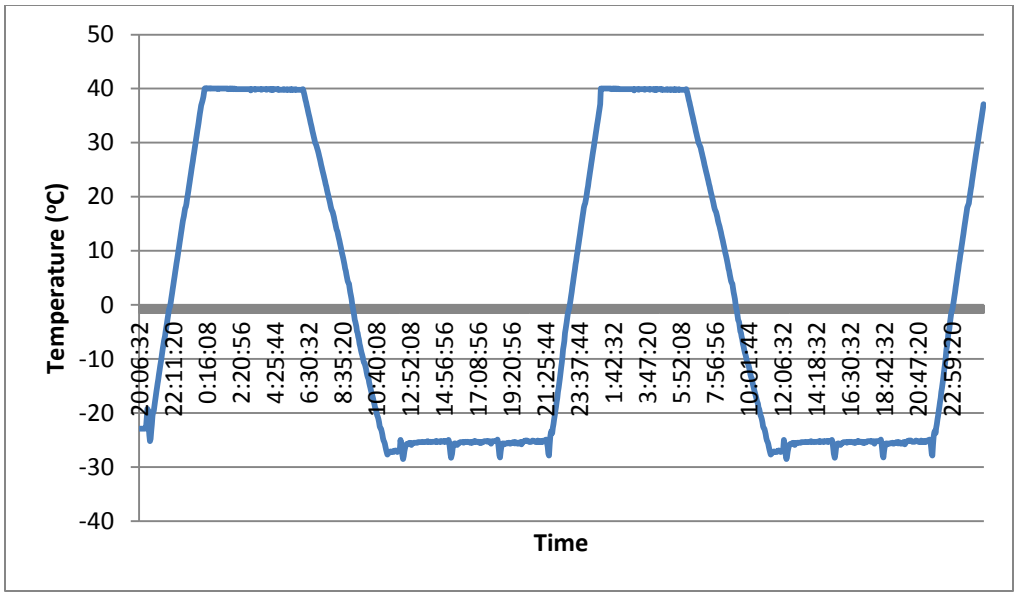

Figure 4.10 Fluctuation of Temperature in 24 hours cycles.

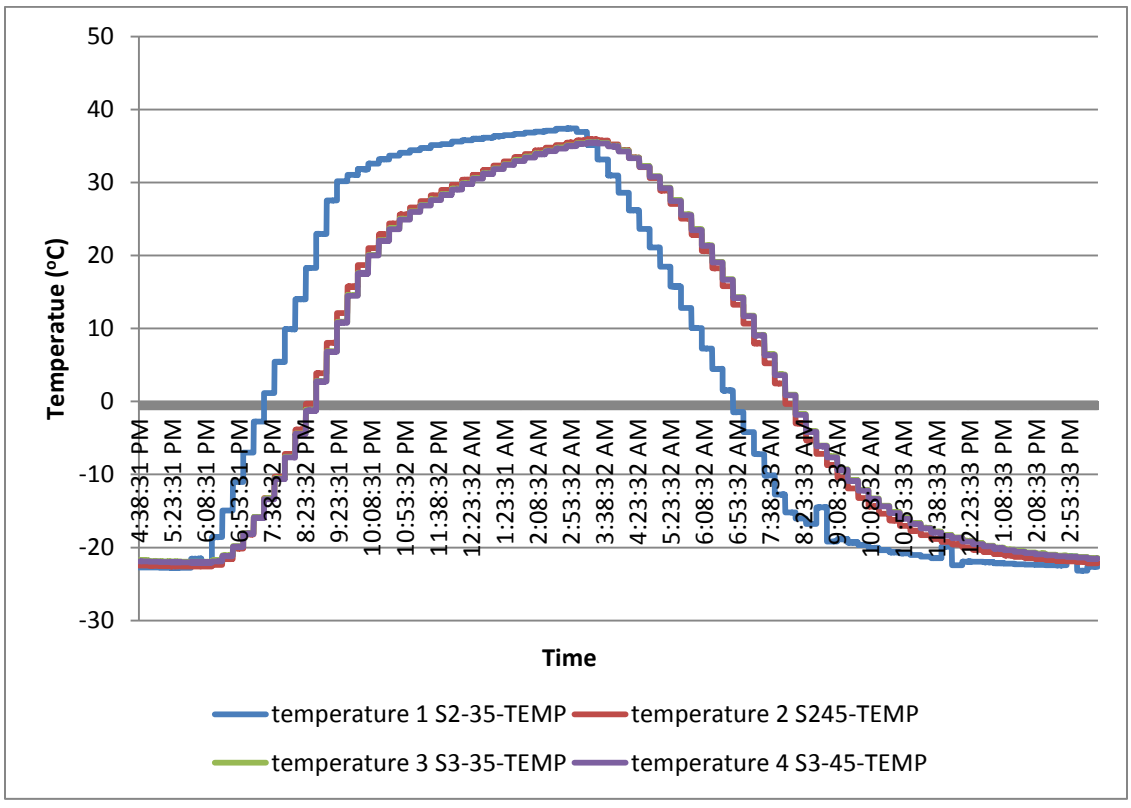

Figure 4.11 Fluctuation of Temperature at the Centre of the Strap in The Environmental Chamber

Figures 4.10 and 4.11 illustrate that the extreme temperatures within the environmental chamber were maintained during a total of three hours to achieve equivalent temperatures at the reinforcing level. Strains were also monitored during the thermal cycling, using electric resistance strain gauges, and as indicated in the figure 4.12, the prestressing levels remained stable with the change of temperature. During the thermal cycling, the beams were randomly checked for damage along their lengths, as well as being superficially inspected at the level of the reinforcement using a 0.1 mm accuracy hand-held microscope. No damage was detected in the straps as a result of exposure to the freeze-thaw cycles.

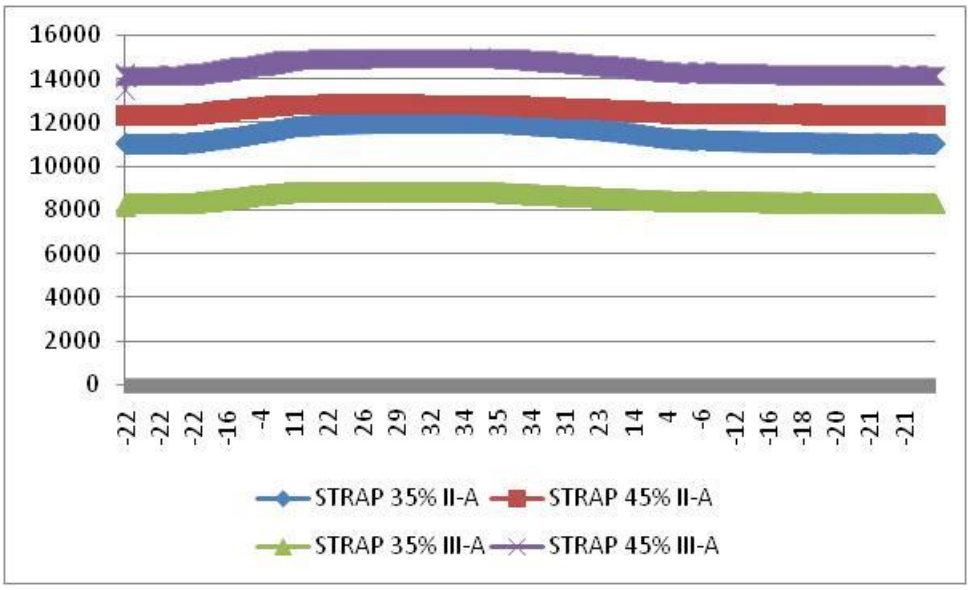

Figure 4.12 Fluctuation of Strains in Straps at varying Temperatures in the Environmental Chamber

4.4 Testing Setup and Instrumentation

After the samples were removed from the environmental chamber, the straps were left for a few days at room temperature. In the meantime, the prestressing setup was shortened to 2.5 m to become the testing layout. The straps were instrumented using PI gauges and an LVDT. The number of PI Gauges were reduced to three placed on the top of the strap to record the cracking of the straps. The Pi gauges were positioned in such a way that the centre of the second PI gauge was aligned with the centre of the strap. The elongation of the strap during the application of load was monitored by an LVDT. The PI gauges and the LVDT were secured by screws cemented to the surface of the beams. Strains, deflection, and load readings were recorded using a 22-channel DAQ system.

4.5 Axial Tests and Results

Each strap was first subjected to 50 cycles of gradually increasing axial load of 50 kN to represent the service load the straps will experience in an actual steel-free bridge deck slab. The strap was tested until failure by applying a monotonically increasing load and observing the crack patterns at each load step. The main objective of the test was to determine the cracking load and compare the behavior of straps of different prestressing levels to those subjected to environmental conditioning.

4.5.1 Cyclic Loading

All the measured load strains for all the straps are presented in Figures 4.13 to 4.21 for set A and in Figures 4.22-4.27 for set B. A random strain gauge was chosen to plot load-strain graph for each of the straps under cyclic loading. As shown in the graphs, the straps showed a linear elastic behaviour with unchanged stiffness throughout testing. Strap 45%

III-A, shown in Figure 4.17 displayed a higher residual strain than the other straps during the cyclic loading. The residual strains of Set B were higher compared to the straps of Set A, which reflects the conditioning of the GFRP for two and half years under sustained loading. Similar behaviour was observed in all of the straps. Figure 4.28 presents the cracking history for the cyclic loading recorded with the PI gauge for Strap 35% I-A for cycles 1, 10, 20, 30, 40 and 50 . No cracks were observed during the cyclic loading. The first crack for all the straps occurred at a load higher than 100 kN.

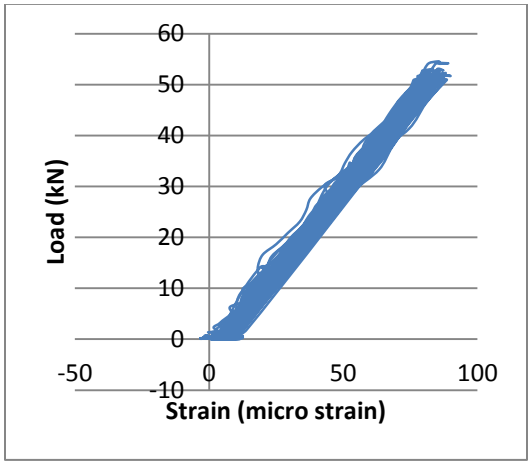

Figure 4.13 Strap 35% I-A

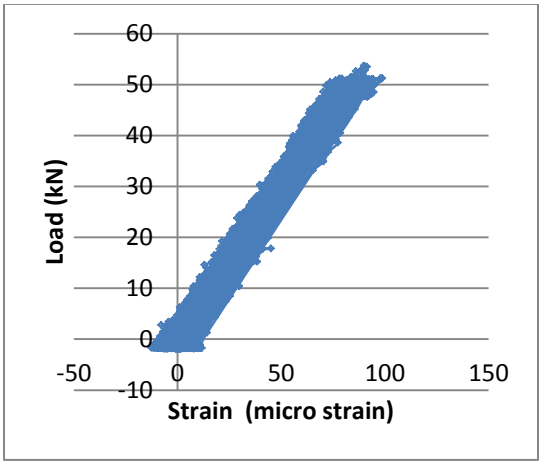

Figure 4.14 Strap 35% II-A

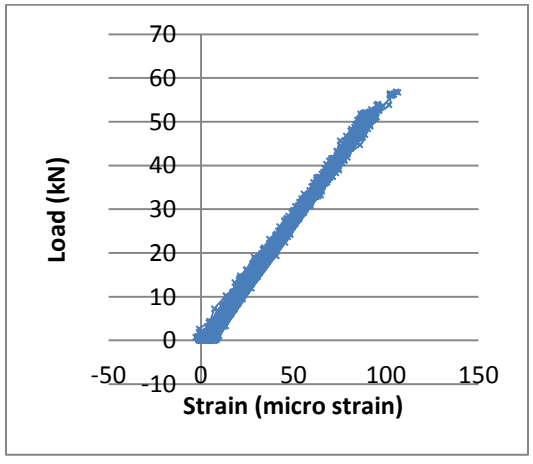

Figure 4.15 Strap 35% III-A

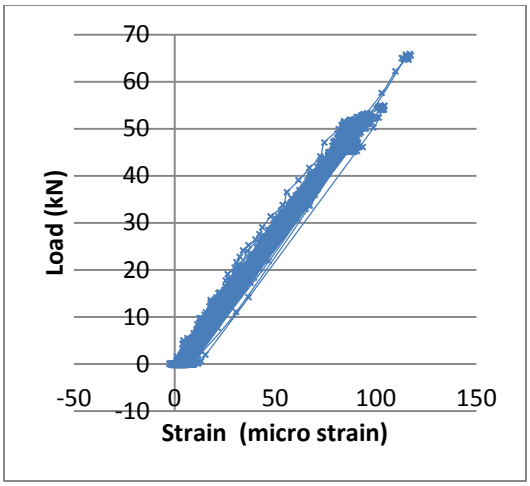

Figure 4.16 Strap 45% I-A

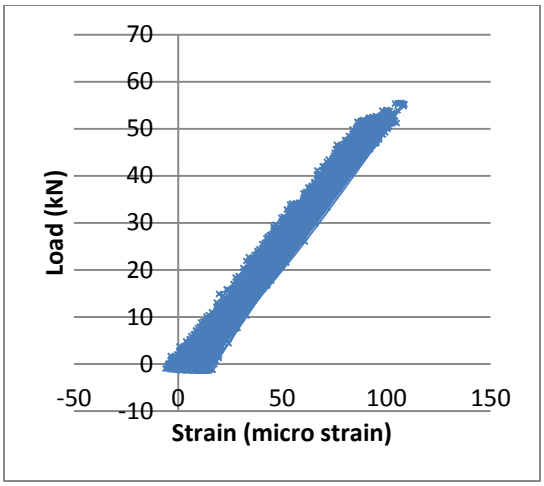

Figure 4.17 Strap 45% II-A

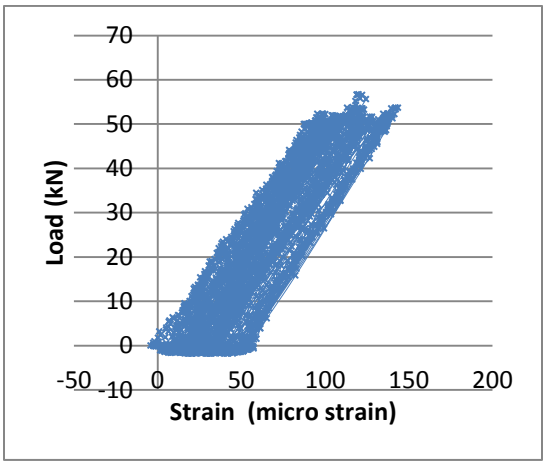

Figure 4.18 Strap 45% III-A

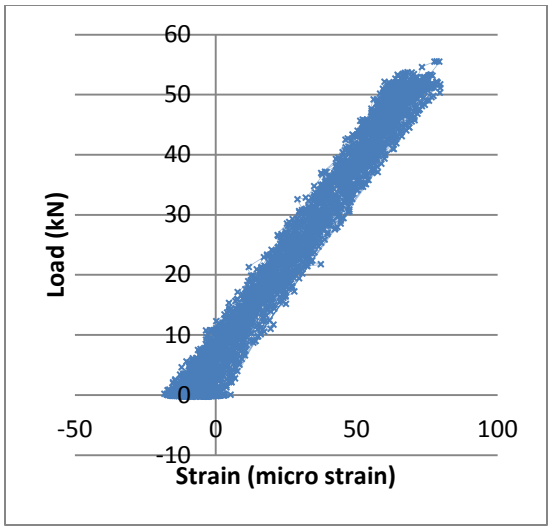

Figure 4.19 Strap 55% I-A

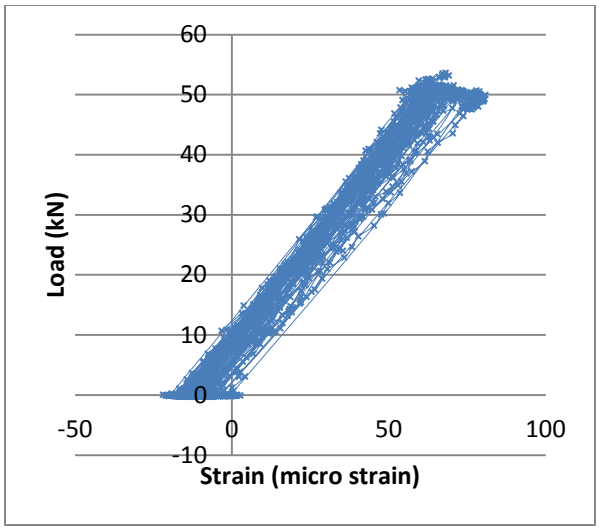

Figure 4.20 Strap 55% II-A

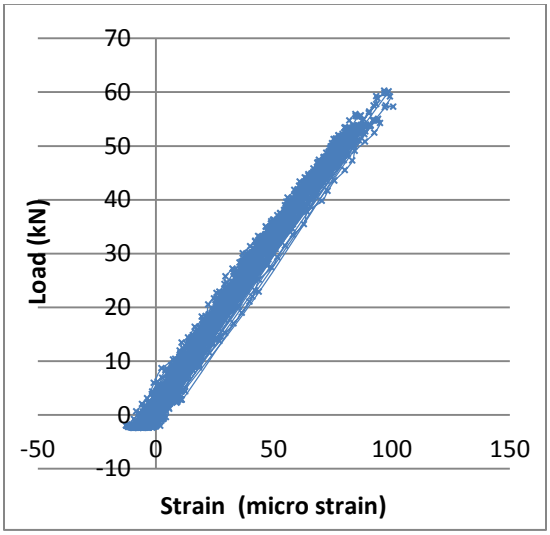

Figure 4.21 Strap 55% III-A

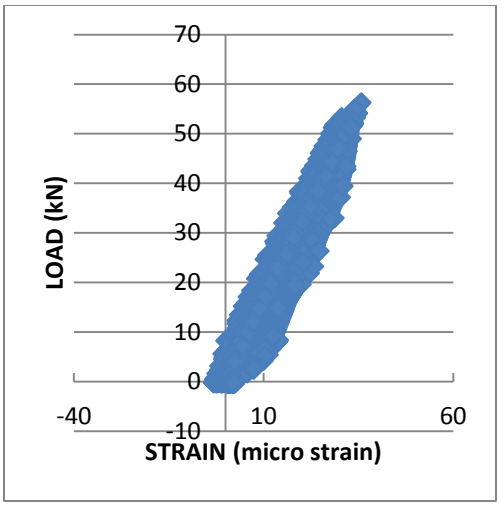

Figure 4.22 Strap 35% I-B

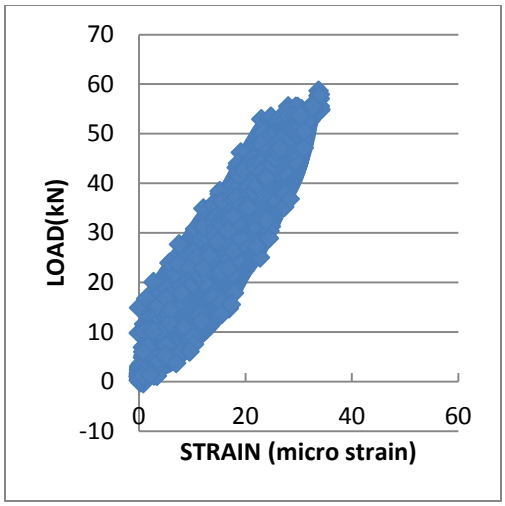

Figure 4.23 Strap 35% II-B

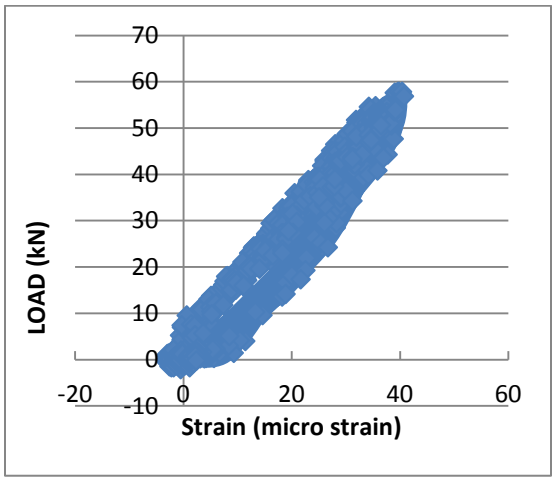

Figure 4.24 Strap 35% III-B

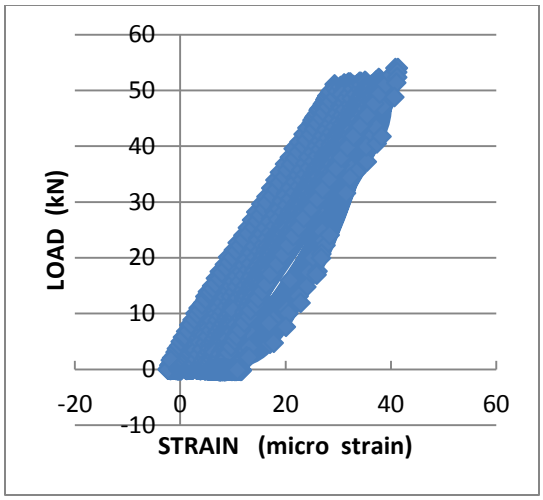

Figure 4.25 Strap 45% I-B

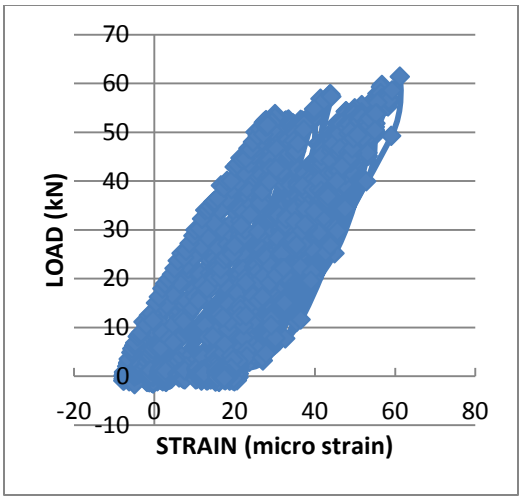

Figure 4.26 Strap 45% II-B

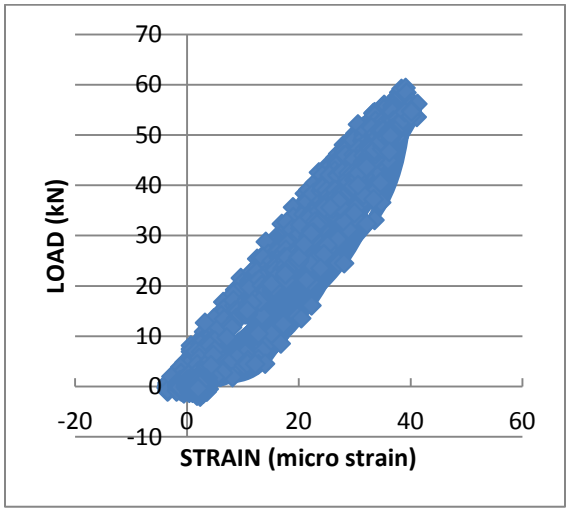

Figure 4.27Strap 45% III-B

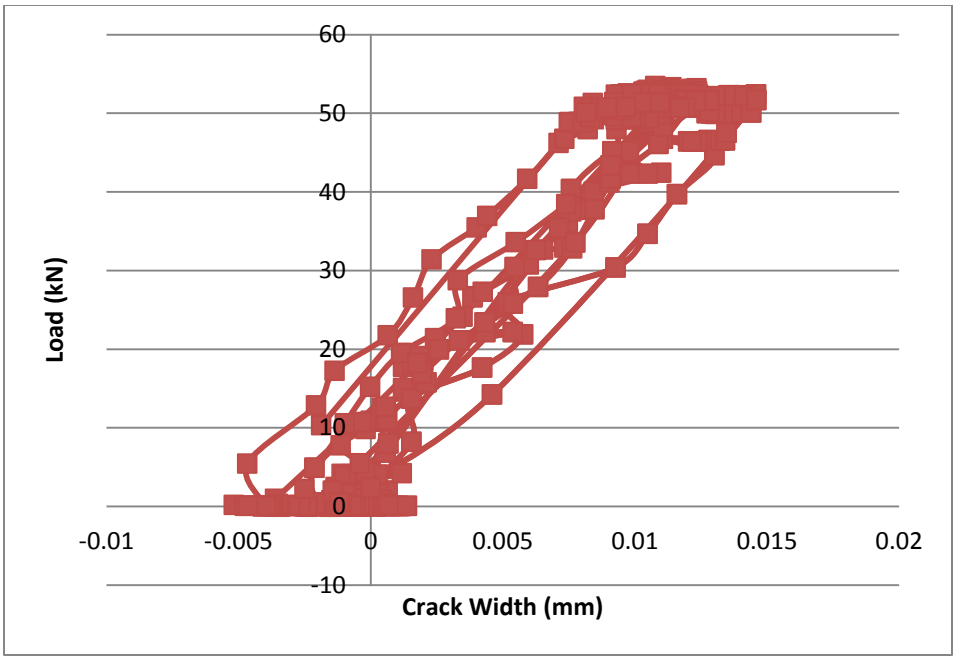

Figure 4.28 Crack Width for Strap 35% I-A

4.5.2 Static Loading

The straps were loaded up to failure by increasing the load incrementally after completing the fatigue study. The cracking load varied depending on the prestressing force after stress release. Straps prestressed at 35% cracked at an average load of 140 kN, while straps prestressed at 45% cracked at 163 kN. The results were also compared to their respective analytical graphs as described by Collins and Mitchell (1997). The variables affecting the results are the prestressing force and environmental conditioning. The prestressing force was estimated based on the last strain reading observed before testing. A sudden drop in the stiffness of the element after cracking, as the concrete becomes inadequate in sharing the stress and the GFRP takes over. At the initial stage of loading the stiffness of the straps is higher until the straps crack and then the stiffness slowly decreases and becomes equal to the stiffness of the bare bars.

4.5.2.1 Static Loading of Set A

Strap 35% I-A failed at the anchorage zone, at 380 mm from the loading end. Both bars slipped at the same location and no rupture occurred at 240kN. Cracking of the strap during the application of the load was at 152 kN, which was closer to the loading end. At failure de-bonding cracks were observed at the anchorage zones with cracking width varying between 0.25 and 0.4 mm. Figure 4.29 and Figure 4.30, are readings of Strap 35% I-A and indicate a typical strain reading and crack width reading for the 35% prestressed straps. On comparing the experimental to the analytical results, the experimental response of the strap was a stiffer than theoretical, as seen in Figure 4.31, which may be contributed to the higher strength of the concrete of the sample to that of the cylenders. Figure 4.32 shows the crack formation in the strap at a load of 200 kN.

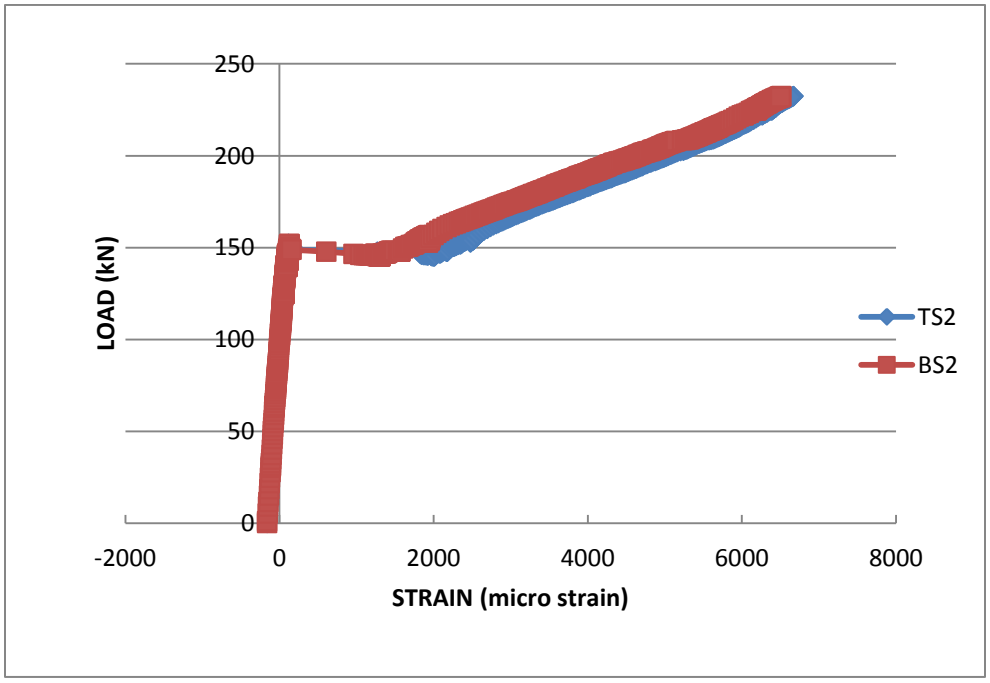

Figure 4.29 Typical Strain Gauge Reading

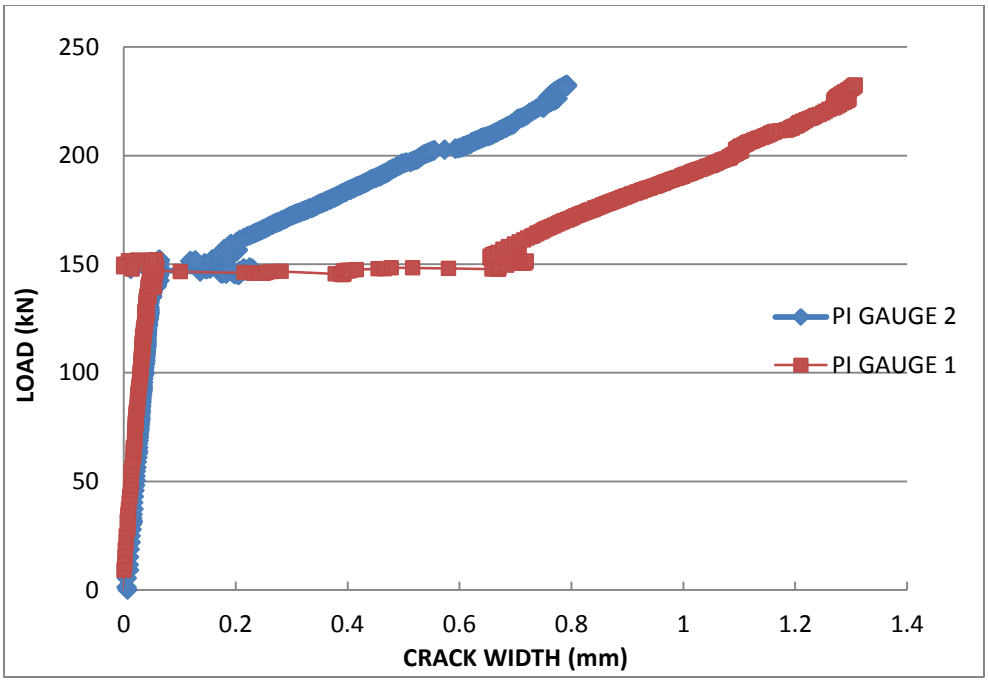

Figure 4.30 Typical Crack Width Reading

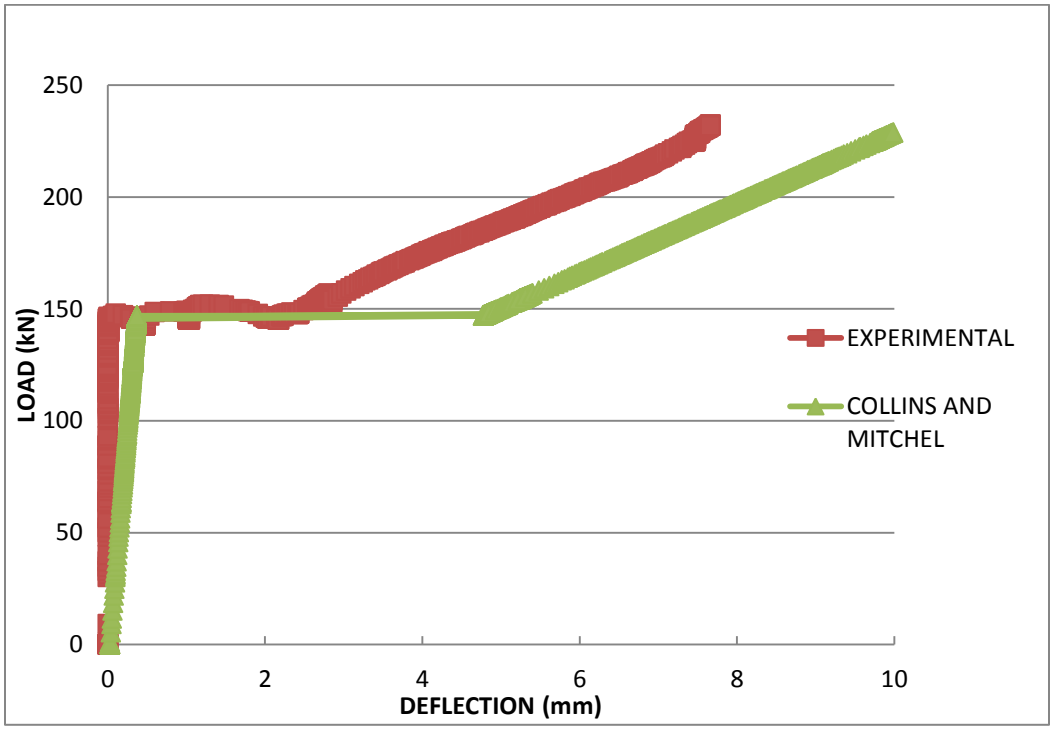

Figure 4. 31 Comparison of the Experimental and Theoretical Behaviour of 35% I-A

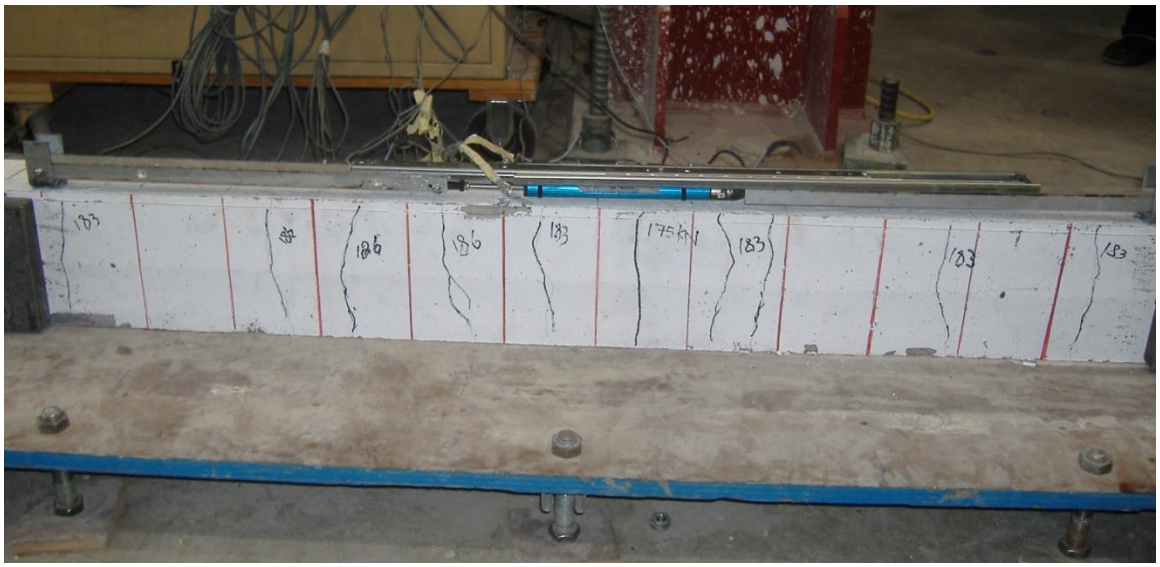

Figure 4.32 Crack Propagation of Strap 35% I-A

Strap 35% II-A had an anchorage failure which occurred at 380 mm from the dead end, where the top bar slipped while the bottom bar ruptured at 230 kN, as seen in Figure 4.33. While placing the plates of the pulling mechanism, a crack of 30 cm by 0.2 mm appeared at the dead end between the two GFRP bars. This crack might have appeared while trying to manipulate the plate to pass through the threaded bars. During the application of load the first crack appeared at 130 kN at the loading end, whereas the failure of the strap occurred at the dead end. De-bonding cracks were observed and ranged between 0.15 and 0.5 mm. The strap had cracked at a lower load than would have been expected in comparison with the experimental results (Fig. 4.34).

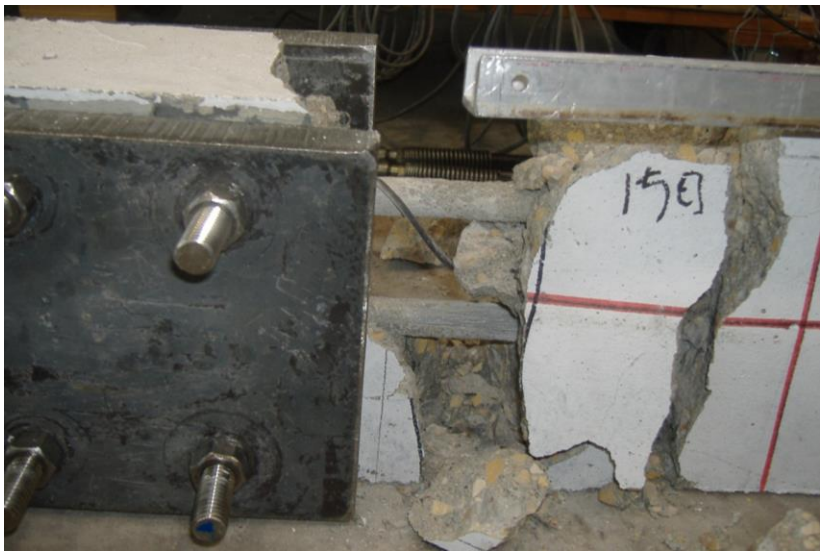

Figure 4.33 Failure Mode of Strap 35% II-A

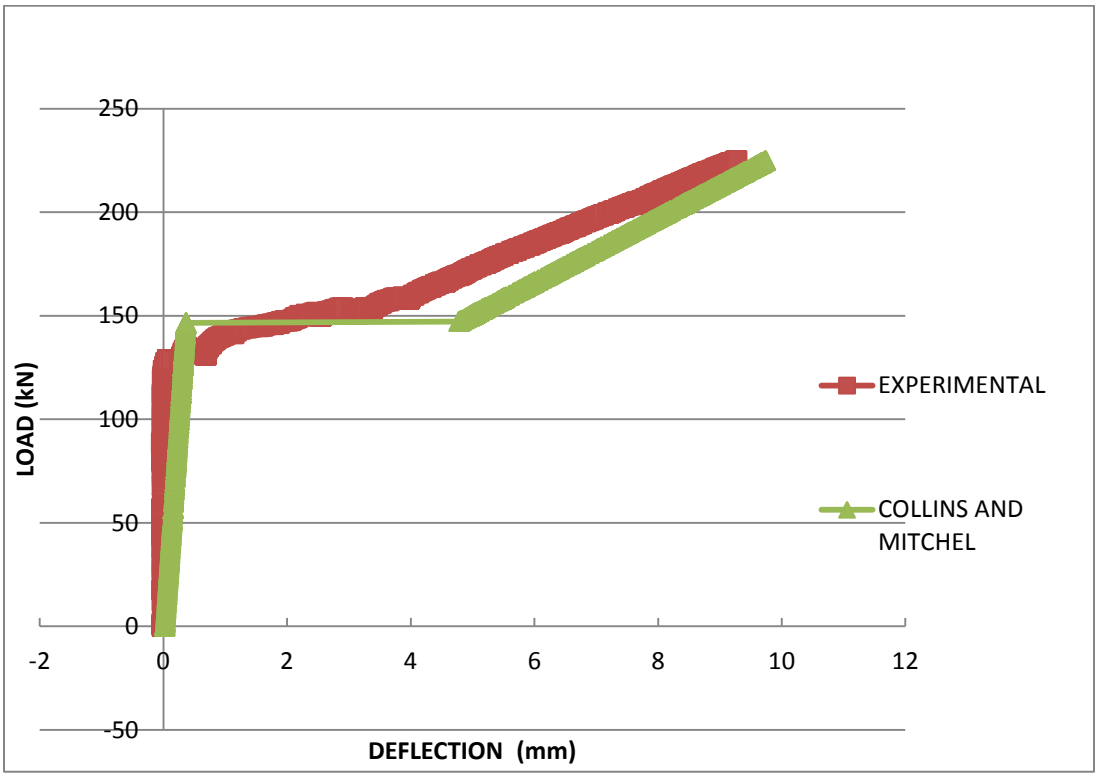

Figure 4.34 Elongation of Strap 35% II-A

Strap 35% III-A first cracked at 150 kN in the center of the strap, and failed through rupture of both bars at the center of the strap at 250 kN, as seen in Figure 5.35. De-bonding cracks could be observed running along the length of the strap with a width varying between 0.1 and 0.5 mm. No cracks were present at the anchorage zone. Figure 4.36 shows comparable stiffness and deflection between the experimental and the analytical results.

Figure 4.35 Failure Mode of Strap 35% III-A

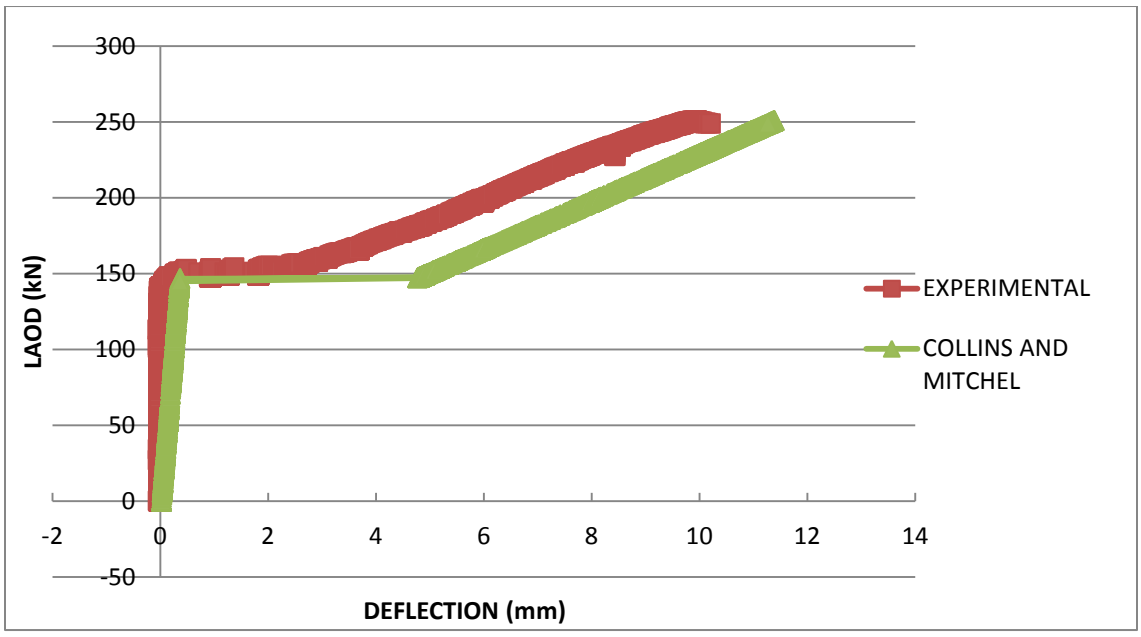

Figure 4.36 Elongation of Strap 35% III-A

Results for 45% straps were very similar to those of 35% straps. Strap 45% I-A had its first crack appear at a load of180 kN, and as the load increased a slip of the top bar occurred, causing more stress to be carried by the bottom bar and rupture at 280 kN, as seen in Figure 4.37. The bottom bar ruptured at 330 mm in the anchorage zone at the dead end. Figure 4.38 shows the sudden slip in the strap and could be observed in the sudden drop of the deflection readings. De-bonding cracks appeared at the dead end with crack width ranging between 0.1 and 0.8 mm at failure.

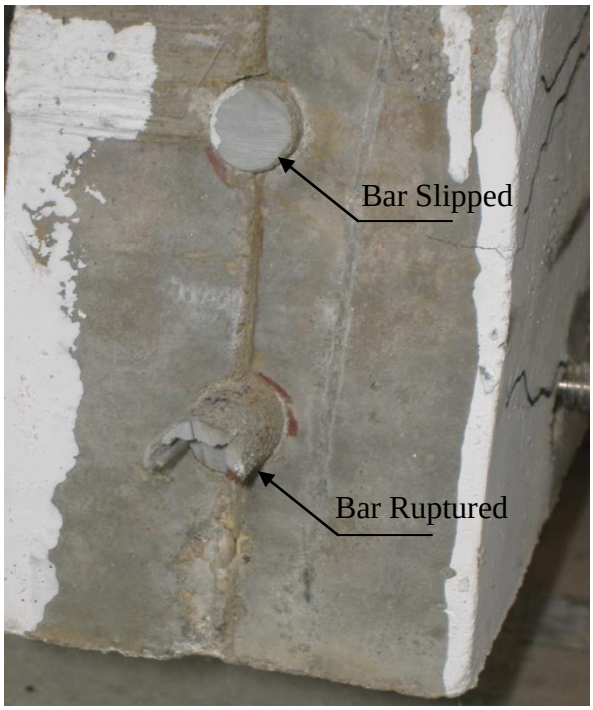

Figure 4.37 Failure Mode of Strap 45% I-A

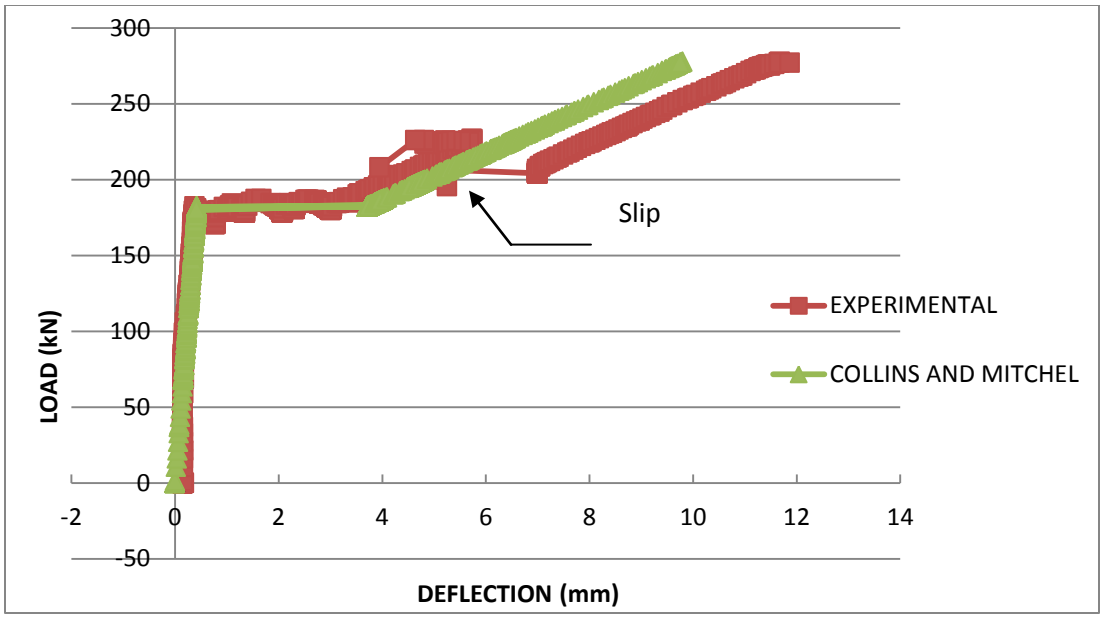

Figure 4.38 Elongation of Strap I at 45%

Strap 45% II-A had its first crack at 173 kN and suffered from slip of both bars, similarly to the first strap; the top bar experienced more slip than the bottom bar causing its rupture at 230 kN, as seen in Figure 4.39. The total deflection was less than the strap should have sustained at higher loads as observed in Figure 4.40. The fluctuations observed in the LVDT reading was because the wire was accidentally stepped on by the wheel of the cart. Failure of the strap occurred at 450 mm from the loading end. De-bonding cracks were present ranging between 0.1 and 0.8 mm.

Figure 4.39 Failure Mode of Strap 45% II-A

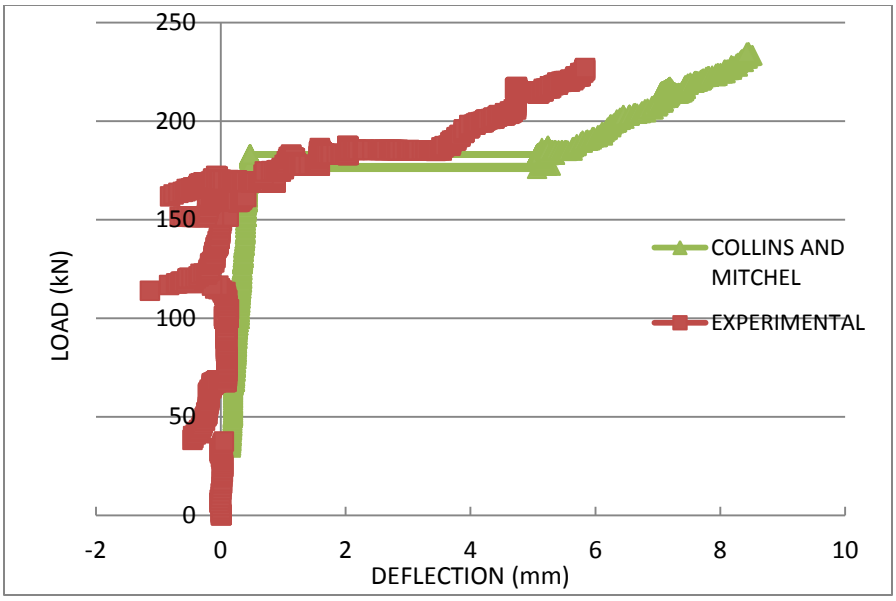

Figure 4.40 Elongation of Strap 45% II-A

Strap 45% III-A cracked at 165 kN and failed at 480 mm from the loading end, where the top bar slipped leading to the rupture of the bottom bar at a load of 225 kN (Fig.4.41). De-bonding cracks were observed along the whole length of the strap ranging between 0.1 and 0.8 mm. Figure 4.42 presents the comparison between the experimental and analytical results.

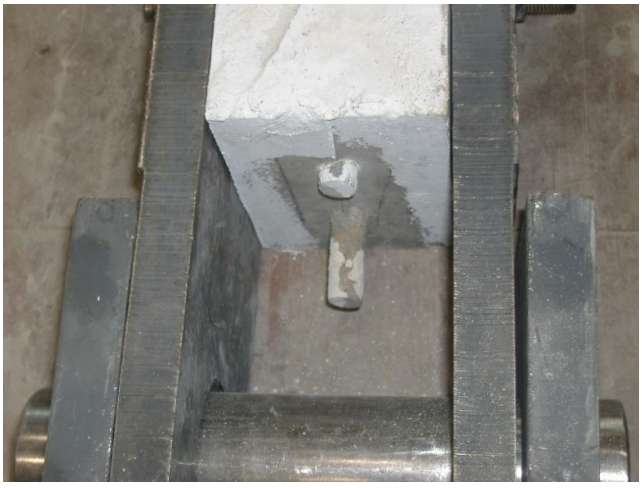

Figure 4.41 Failure Mode of Strap 45% III-A

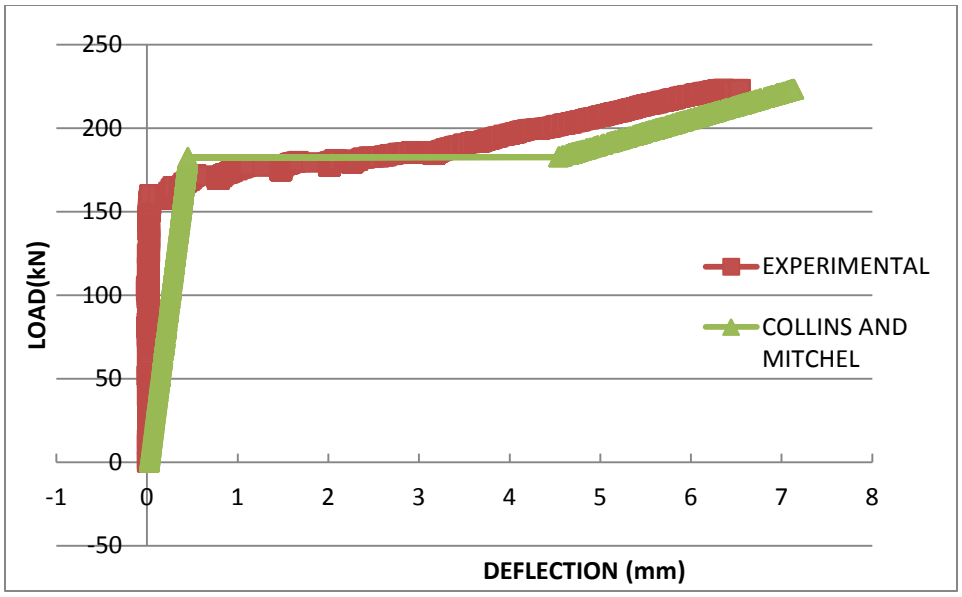

Figure 4.42 Elongation of Strap 45% III-A

All three straps experienced a single crack, then rupture of both bars without slip as seen in Figs. 4.43– 45). Strap 55% I-A failed at the center of the strap by rupture of both bars at 210 kN (Fig. 4.43). The de-bonding cracks appeared along the length of the strap with crack width ranging between 0.1 and 0.9 mm. Strap 55% II-A failed by rupture of both bars at 200 kN at 500 mm from the loading end; these de-bonding cracks ranged between 0.1 and 0.75 mm. Strap 55% III-A had a crack appearing along the length of the strap during the manipulation of the plate for the pulling mechanism. The crack prompted the strap to fail at a lower load of 70 kN. The experimental results (Fig.4.46) illustrate that the straps elongated for less than 1 mm, that the failure was sudden and with very little warning, and that the straps had very low elongation.

Figure 4.43 Failure Mode of Strap 55% I-A

Figure 4.44 Failure Mode of Strap 55% II-A

Figure 4.45 Failure Mode of Strap 55%III-A

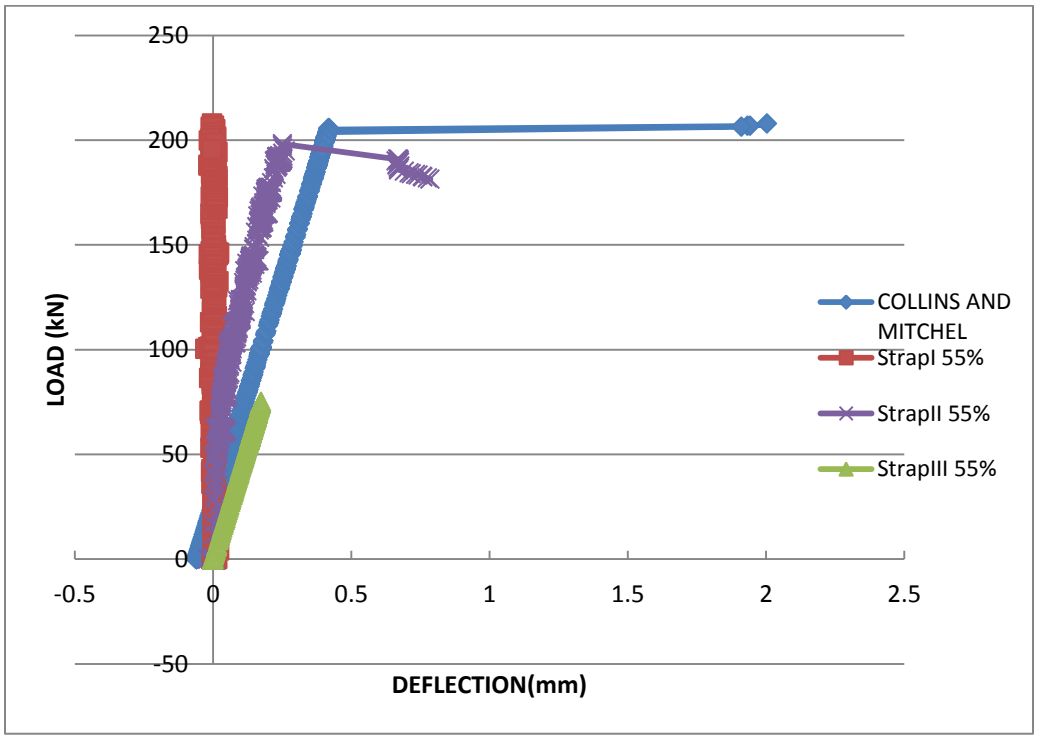

Figure 4.46 Elongation of Straps Prestressed at 55%

The straps did not crack during the cyclic testing under 50 kN force, but during the ultimate loading the straps exhibited a characteristic sequence and crack pattern. The occurrence and development of cracks was closely monitored during the application of the axial load. The straps prestressed at 35% and 45% of the ultimate strength exhibited different cracking loads for all the straps: the straps prestressed at 35% cracked at 150, 130 and 150 kN, while straps prestressed at 45% cracked at 180, 173 and 165 kN. The cracking patterns as well as the widths were similar ranging between 0.1 and 0.5 mm for straps prestressed at 35% and 0.1 and 0.8 for straps prestressed at 45%. As the straps were close to failure, a transverse crack appeared indicating bond failure. When comparing the results of the control sample to the weathered straps, the strain readings measured along the bars among all straps were consistent. This was deemed sufficient evidence to conclude that the bond strength was not affected by the environmental conditioning. Once the straps cracked there was a sudden drop in the stiffness of the member at the location of cracking, as the concrete becomes ineffective in sharing the stress and the GFRP takes over; however, the effect of tension stiffening is very visible at the uncracked sections. The straps prestressed at 55% of the ultimate load had a distinctive mode of failure where a single crack appeared and then rupture of the bars occured, demonstrating that the cracking load is the same as the ultimate load. The material's behaviour changed when the GFRP bars were stressed at a high sustained load of 55% of the ultimate strength and failed due to creep. In this case the failure process of the members was directly affected by the sustained load alone. Figures 5.47 - 47 present the crack pattern and failure mode of all the straps tested in this research.

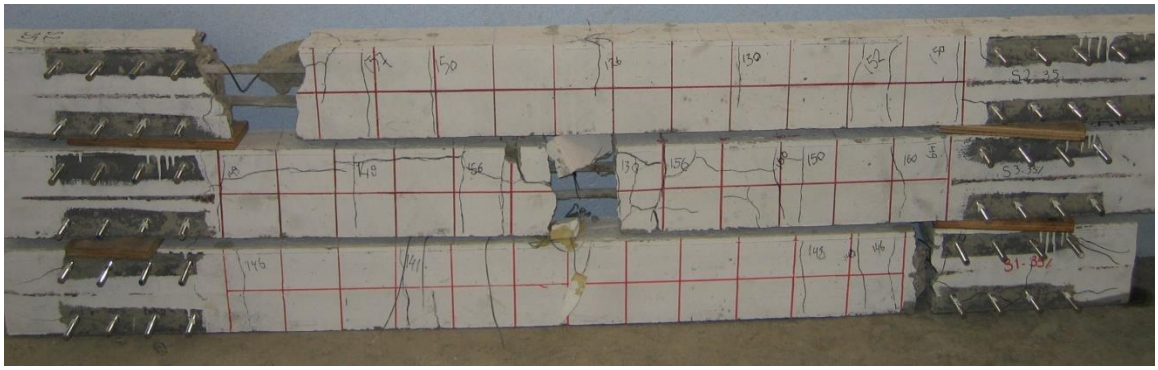

Figure 4.47 Crack Pattern and Mode of failure of Straps Prestressed at 35%-A

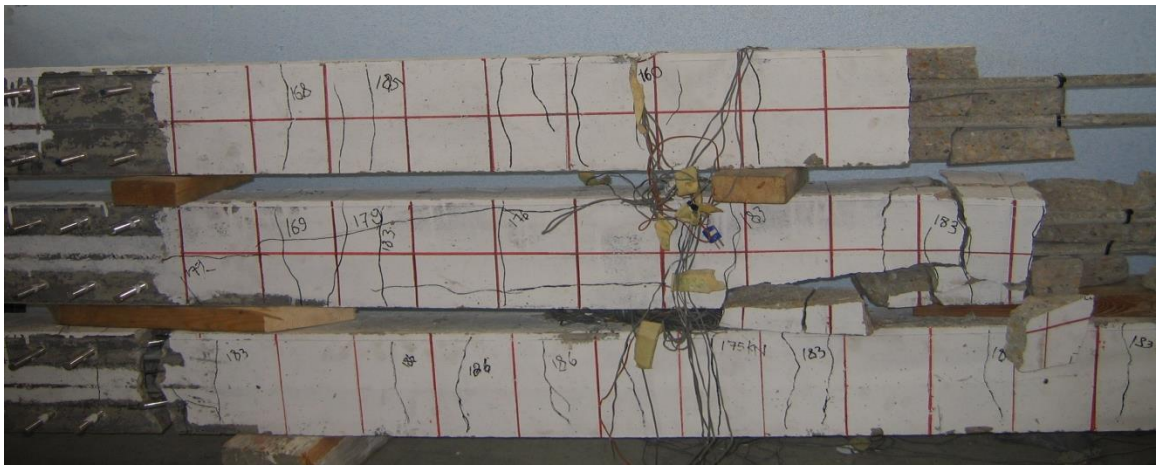

Figure 4.48 Crack Pattern and Mode of failure of Straps Prestressed at 45%-A

Figure 4.49 Crack Pattern and Mode of failure of Straps Prestressed at 55%-A

4.5.2.2 Static Loading of Set B

Set B of the straps was tested two and a half years after casting. A total of three straps prestressed at 35% and 45% prestress level were tested. Strap 35% I-B experienced first crack at 125 kN close to the dead end, but it did not go through the section and was not registered on the strain gauges or LVDT, therefore this reading and any similar cracks at the ends were ignored as the recorded first crack. This crack was most likely due to the stress concentration at the end the strap where the large anchorage plates were attached. The first crack that appeared at the center of the strap was then considered as onset of cracking. The load at which the first crack occurred were deduced from the LVDT and strain gauge data. Cracks propagated with the increase of load until rupture of both bars close to the pulling mechanism of both bars at 280 kN. The failure of the strap could be described as being explosive with concrete blocks were scattered and the ruptured bars exposed. Debonding cracks were observed running along the top bar and having a width of 2.5mm. Figure 4.50 and 4.51 present a typical strain and crack width readings of the straps plotted against load. Figures 4.52 presents the total elongation of the strap when the load was applied.

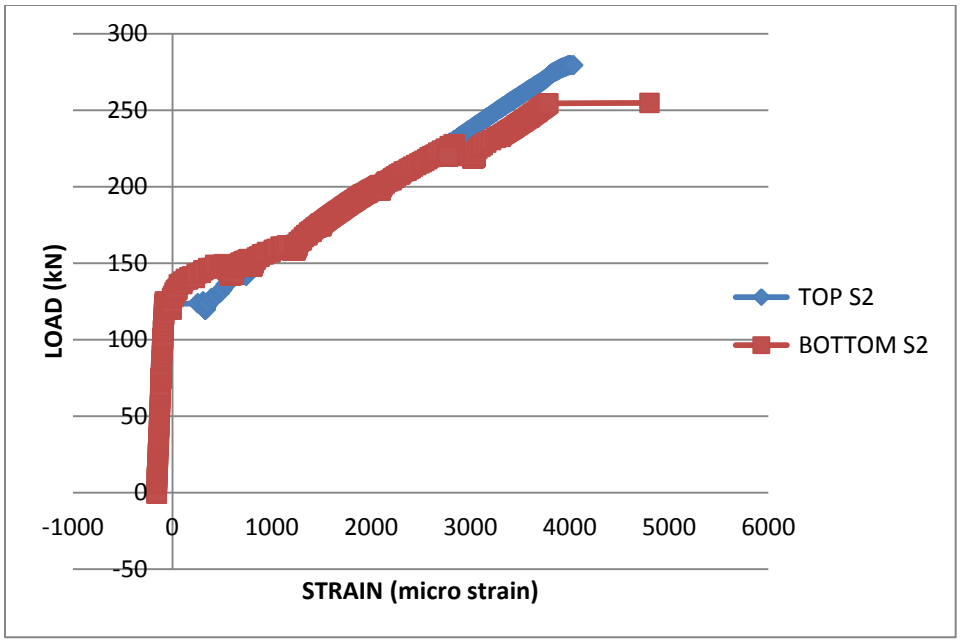

Figure 4.50 Typical Strain Gauge Reading

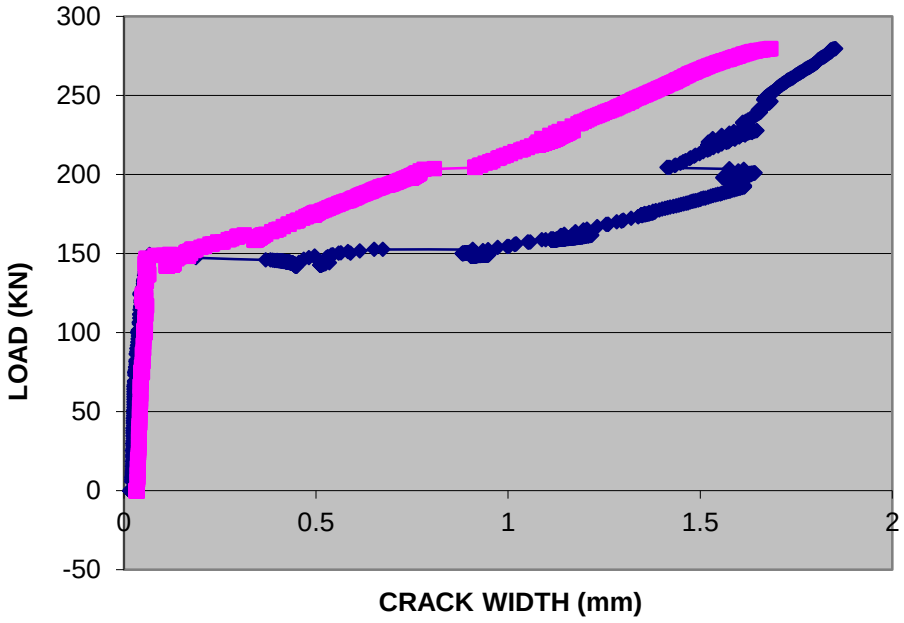

Figure 4.51 Typical Crack Width Reading

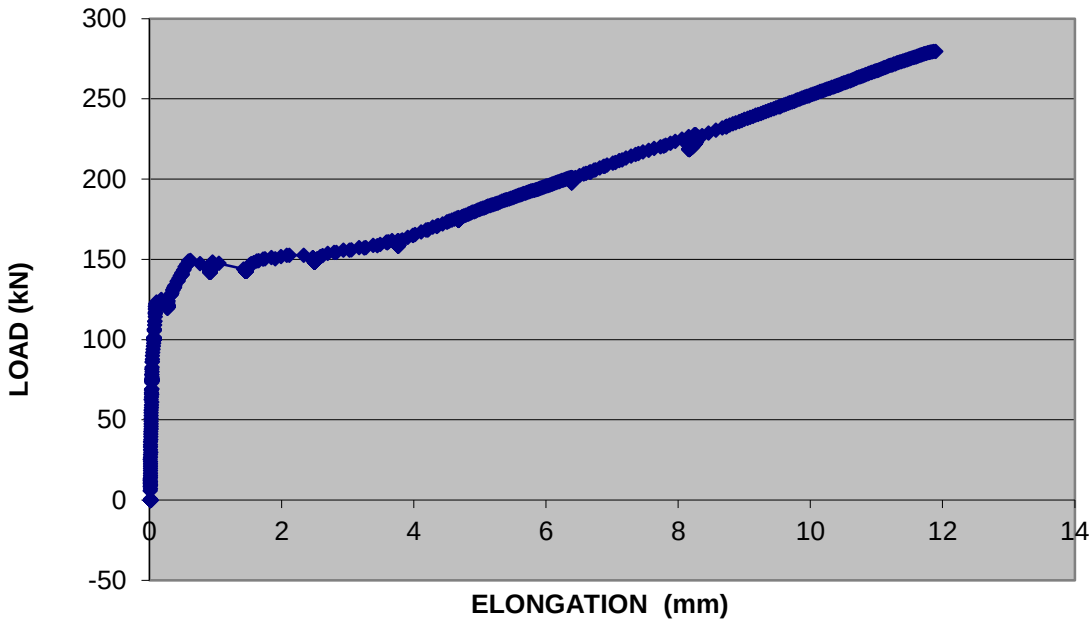

Figure 4.52 Elongation of Strap 35% I-B

Figure 4.53 Failure Mode of Strap 35% I-B

Strap 35% II-B experienced its first crack at 144 kN close to center , the cracking pattern could be observed on Figure 4.54. The strap failed at a load of 271 kN by the rupture of both bars at the center of the strap. The failure was characterized as explosive, simillar to Strap 35% I-B. Figure 4.55 presents almost equal stiffness when comparing the

experimental results to the analytical data. The stiffness of the strap was high and is the most governing criterea for the straps when used in steel- free bridge deck slab.

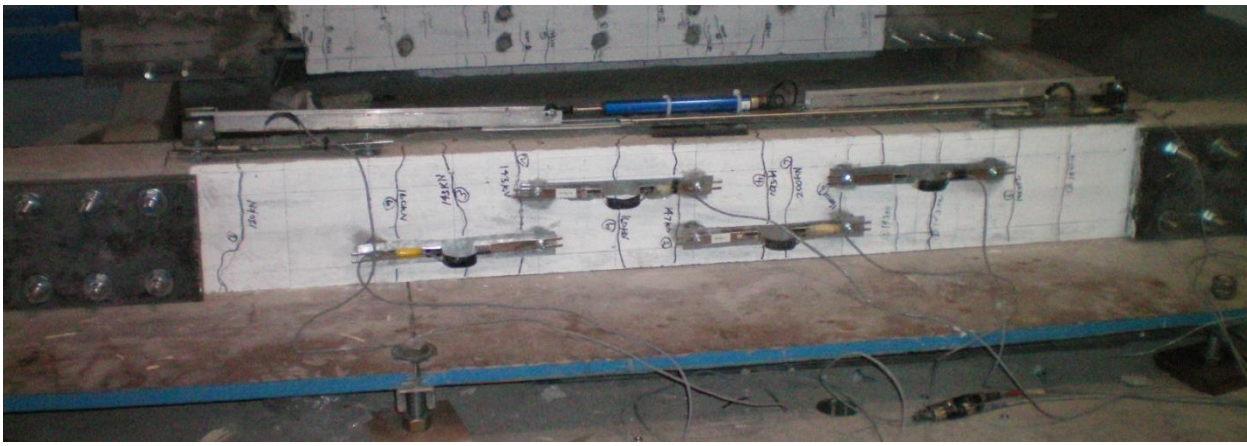

Figure 4.54 Crack propagation of Strap 35% II-B

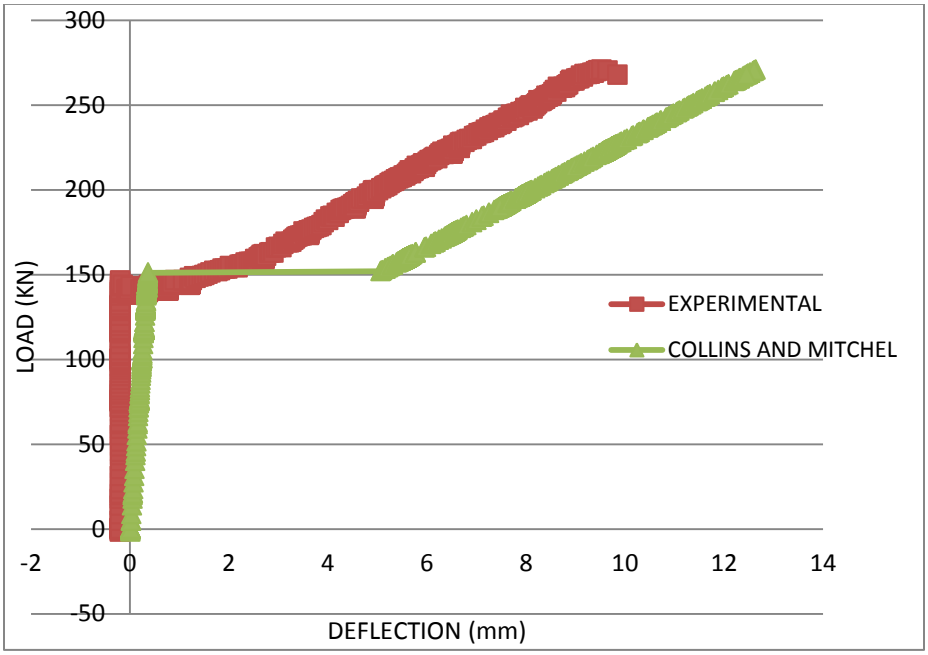

Figure 4.55 Elongation of Strap 35% II-B

Strap 35% III-B suffered from anchorage failure by slippage of both bars at the end of the pulling mechanism as seen in Figure 4.56. the strap first cracked at 143 kN and failed at 276 kN. Slip of the bars can be observed in Figure 4.57.

Figure 4.56 Failure Mode of Strap 35% III-B

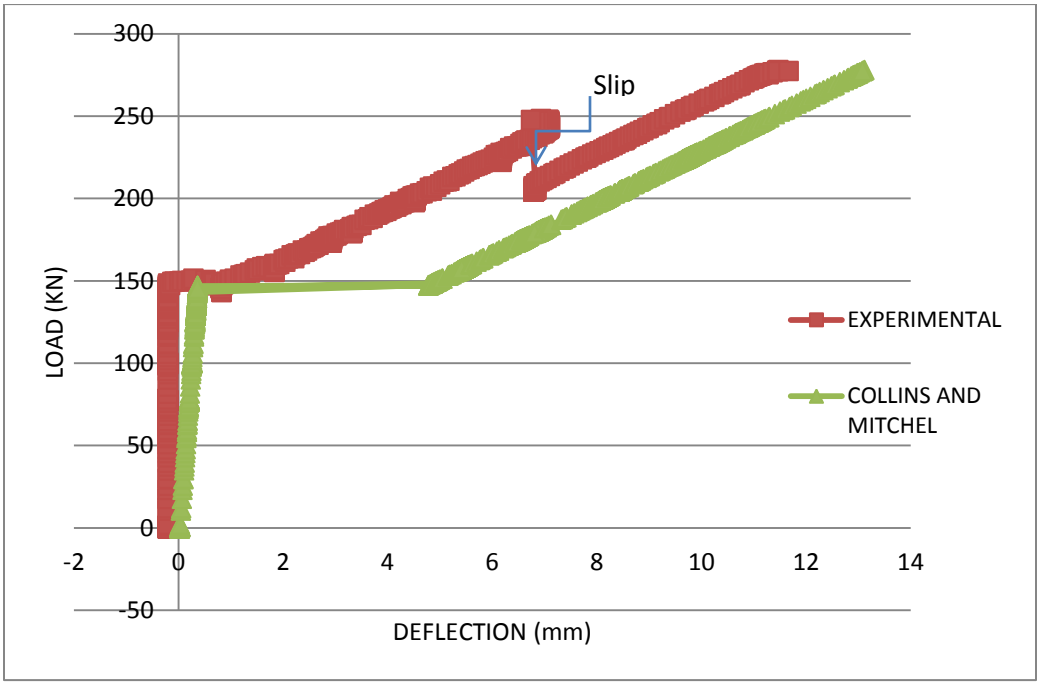

Figure 4.57 Elongation of Strap 35% III-B

Strap 45% I-B first cracked at a load of 156 kN and a crack pattern as presented in Figure 5.58. The crack width that the strap has experienced ranged between 0.4-1.5mm and a total elongation of 10.5mm (Figure 4.59). The strap suffered from anchorage failure at the dead end, where there was a slip in the bottom bar forcing the rupture of top bar as seen in Figure 4.60

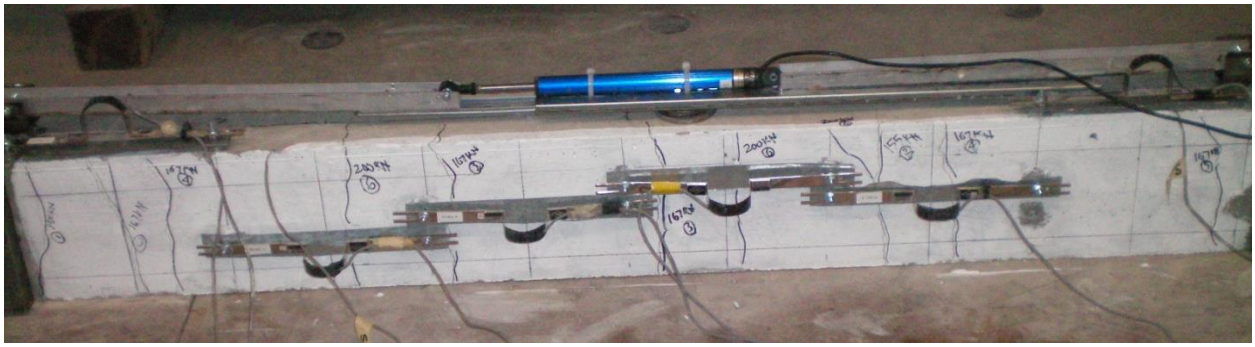

Figure 4.58 Crack Pattern of Strap 45% I-B

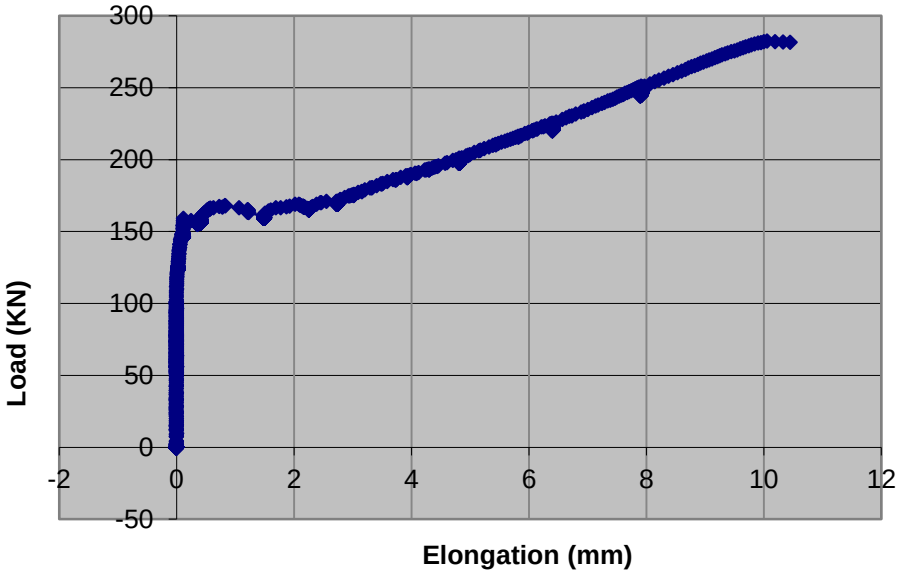

Figure 4.59 Elongation of Strap 45% I-B

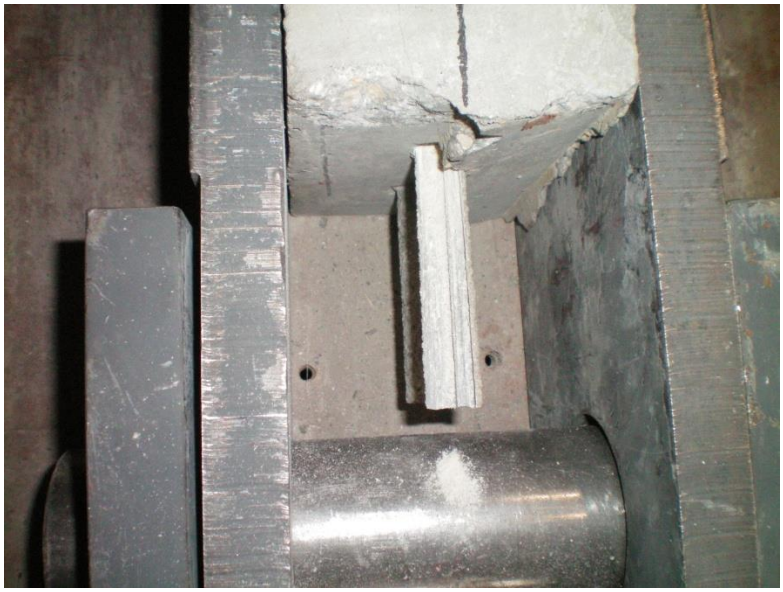

Figure 5.60 Failure Mode of Strap 45% I-B

Strap 45% II-B cracked at a load of 155 kN and suffered an anchorage failure at 273 kN, similar to the first strap (Figure 4.61). The stiffness of the strap is higher than that in the experimental analysis although the total deflection was less than the strap should have sustained, as observed in Figure 4.62.

Figure 4.61 Failure Mode of Strap 45% II-B

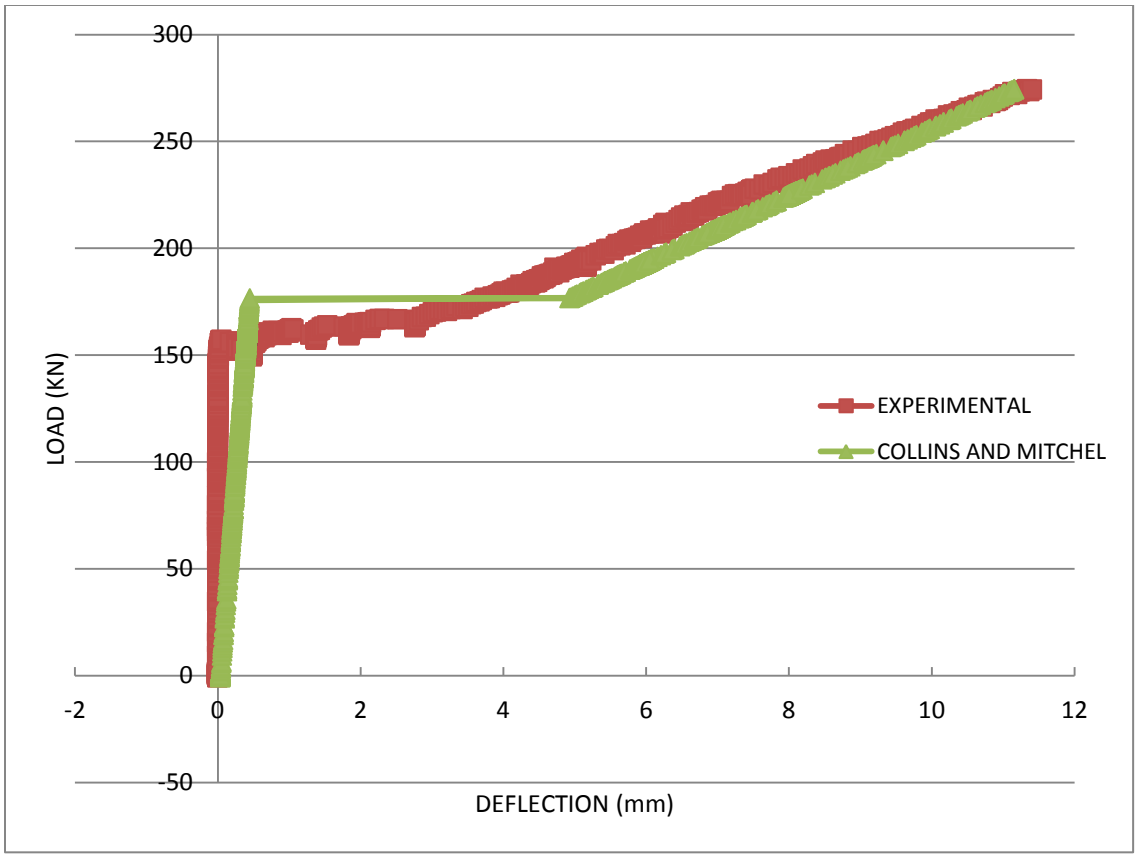

Figure 4.62 Elongation of Strap 45% II-B

Strap 45% III-B cracked at a load of 154 kN and failed by rupture of both bars at 273 kN at the dead end. A horizontal crack appeared while manipulating the pulling mechanism into the threaded rods at the dead end reaching 86 cm in length as seen in Figure 4.63. During the application of load horizontal cracks identifying the de-bonding of the top bar appeared and reached 2.8 mm in width, as for the vertical crack width ranged between 0.5 and 1.7 mm.

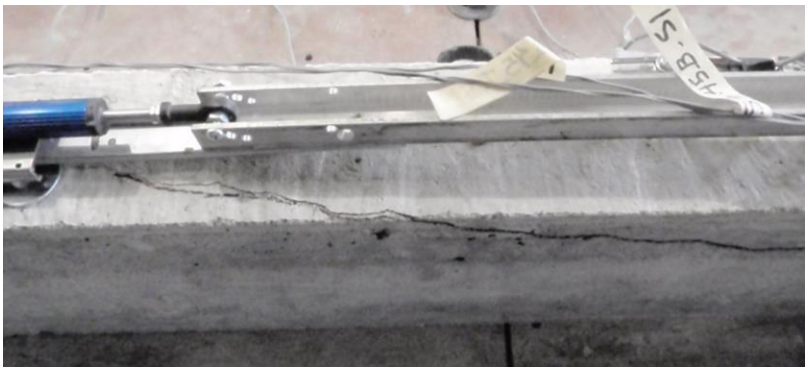

Figure 4.63 Horizontal Cracks on Strap 45% III-B

Figure 4.64 Failure Mode of Strap 45% III-B

The straps in Set B did not crack during the cyclic loading under 50 kN force. The occurance of the cracking during the application of the static loading was closely monitored, and it exhibited similar crack patterns to what was previously observed in Set A. Transverse de-bonding cracks were observed as the straps were close to failure. The conditioned straps and the control samples all cracked and failed at the same load, although the failure modes were different as seen in Figures 4.65-4.66. The data collected

also demonstrated great similarities when comparing those of the control sample to those of the conditioned sample.

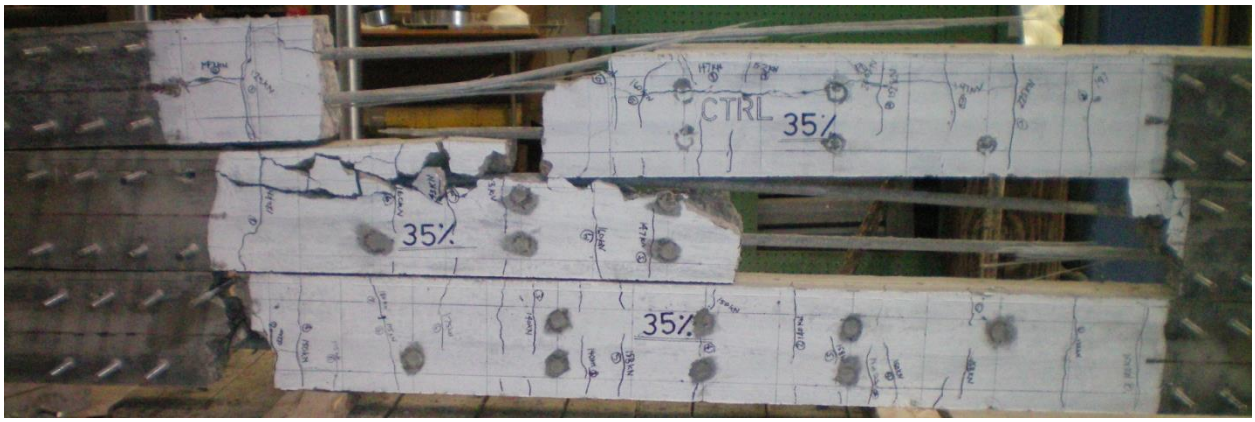

Figure 4.65 Crack Pattern and Mode of failure of Straps Prestressed at 35%-B

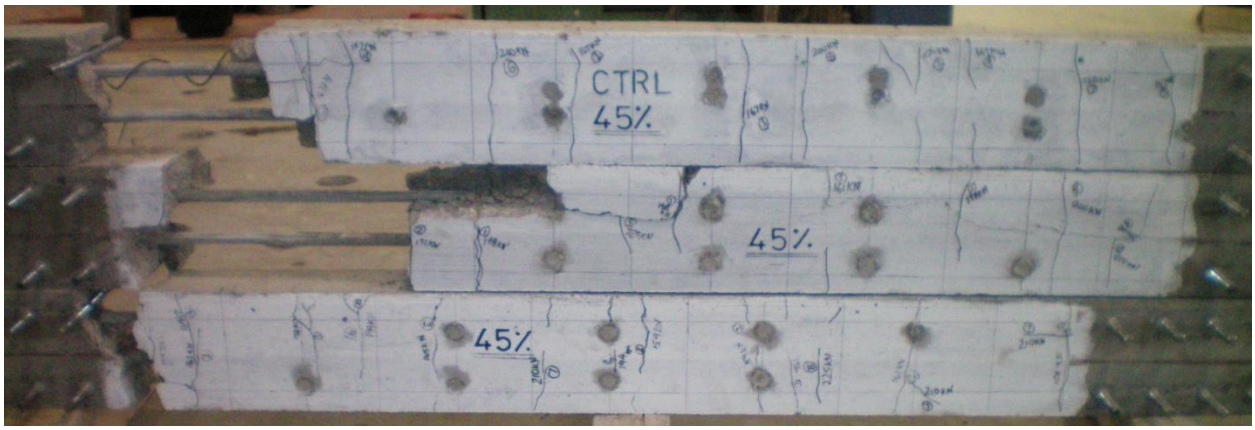

Figure 4.66 Crack Pattern and Mode of failure of Straps Prestressed at 45%-B

When comparing the results of the straps of Set A and Set B presented in Tables 5.1 and 5.2 the following observations can be made:

- The cracking load decreased with exposure to the environment.
- The load at cracking increased with increase of prestressing level.
- The load at failure has increased for the straps prestressed at 35% and 45% and that could be contributed to the increase in concrete strength with time and the loss in prestressing.
- It can be deduced from the average load at cracking of Set A to set B is that there was a loss of prestressing of 4% for the straps prestressed at 35%, and is considered reasonable for long term losses. As for the straps prestressed at 45% there was losses of up to 11%, which is higher than expected.

Table 5.1 Loads at Cracking and Failure for Set A and B

	Pcr	Pultimate
Strap 35%I-A	150	240
Strap 35%II-A	130	230
Strap 35%III-A	150	250
Strap 45%I-A	180	280
Strap 45%II-A	173	230
Strap 45%III-A	165	225
Strap 35%I-B	125	280
Strap 35%II-B	120	271
Strap 35%III-B	132	276
Strap 45%I-B	150	280.3
Strap 45%II-B	156	273
Strap 45%III-B	148	272.5

Chapter 5

Conclusions and Recommendations

This study has shown that the prestressing limit of 25% of the ultimate strength of GFRP indicated in Canadian Highway Bridge Design Code (CHBDC, 2006) is conservative. This research provides no sufficient evidence to increase the prestressing limit to a higher value, as more research is needed to study the creep of GFRP.

Two sets of three straps for each prestressing level of 35%, 45% and 55% were cast on April 2 and on May 30, 2008. The first set, Set A sustained thermal conditioning of 75 cycles ranging between -23 ^{o}C and 40 ^{o}C , as set B was tested under the same thermal conditioning for 50 cycles, two and a half years after casting. Each set had comparable results with its control sample, but when comparing the two sets together prestressing losses within two and a half years where high for the straps pr-stressed at 45%.

The following conclusions have been drawn from the research study reported in this thesis:

- The coupler designed for stressing the two GFRP bars at once proved to function well in and kept the bars stressed without slip during the prestressing process, and it ensured that both bars would have the same stress.
- Use of coils prevented splitting of the concrete cover after the release of prestressing.
- The weathered beams were regularly inspected with the use of a 0.1 mm accurate hand-held microscope for damage during thermal cycling and it was apparent that no damage occurred in the transfer regions of the straps.
- It is clear from comparing the data of control samples to that of the weathered straps that the deviation of results was not significant enough to suggest a noticeable trend in bond strength.

- Strap prestressed at 45% exhibited 11% loss in prestressing within two and a half years, which indicates that the stress is too high for the GFRP bar..
- Straps prestressed at 55% of the ultimate strength failed due to creep rupture under sustained loading.

The following are recommendations for future studies involving FRP tendons and transverse confinement for steel-free bride deck slab:

- Further studies are needed to study the long-term creep of GFRP when prestressed at 35%.
- More samples needs to be constructed for future studies and tested in 10-15 years and observed under the SEM (Scanning Electron Microscope) and other micro-structural analysis testing procedures for degradation of the fibre/matrix interface.
- The current research ignored the influence of cyclic loading while in the environmental chamber and of testing the straps at different temperatures. Applying loads during softening or hardening of the resin and testing for degradation of the GFRP in the concrete environment would produce a better representation.
- A fatigue analysis of the prestressed concrete straps needs to be tested quantitatively.
- Testing a steel-free bridge deck slab under dynamic loading and confined by the means of GFRP prestressed concrete straps that have been placed under environmental conditioning.

References

AlMusallam, T., Al-Salloum, Y. A. Durability of GFRP Rebars in Concrete Beams under Sustained Loads at Severe Environments. *Journal for Composite Materials.* 2006;40:7:623-637.

ASTM E- 1512 Standard Test Method for Testing Bond Performance of Adhesive-Bonded Anchors. (1993). *ASTM,* 100 Barr Harbor Drive, West Conshohocken, PA 19428.

ASTM C- 39C 39m-99. Standard Test Method for Compressive Strength of Cylendrical Concrete Specimens. (1993). *ASTM,* 100 Barr Harbor Drive, West Conshohocken, PA 19428.

ASTM C- 143/C 143M-98. Standard Test Method for Slump of Hydraulic Cement Concrete. (1993). *ASTM,* 100 Barr Harbor Drive, West Conshohocken, PA 19428.

ASTM C- 496-96 Standard Test Method for Splitting Tensile Strength of Clylendrical Concrete Specimens . *ASTM,* 100 Barr Harbor Drive, West Conshohocken, PA 19428.

Bakht, B., & Agarwal, A. C. (1993). *Deck slabs of skew Girder bridges.* Paper presented at the CSCE Annual Conference for Bridge and Structural Engineering, Fredericton, NS.

Bakht, B., & Lam, C. (2000). Behavior of transverse confining systems for Steel-free Bridge Decks. *Journal of Bridge Engineering* , 139-147 Is there a volume number or issue number? .

Bakht, B., & Mufti, A. A. (1998). Five steel-free bridge decks in Canada. *Journal of the Internatonal Association for Bridge and Structural Engineering (IABSCE)* , 8(3), 786-789.

Bakht, B., & Mufti, A. A. (1996). FRC deck slabs without tensile reinforcement. *Concrete International* , 18(2), 514-530.

Bank L.C., Gentry, T.R., Barakatt, A., Prian, L., Wang, F., Mangla, S.R. Accelerated Aging of Pultruded Glass/ vinyl ester rods. *Proceedings of the 2nd International Conference on the Fiber Composites in Infrastructure, ICCI* 1998;2:423-437.

Banthia, V. (2003). *Transverse Confinement of Steel Free Deck Slabs By Prestressed Concrete Straps.* Master of Science disertation. Winnipeg: Universtiy of Manitoba..

Beal, D. B. (1982). Load Capacity of Concrete Bridge Decks. *ASCE Journal of the Structural Division* , 108 (ST4): 814-832.

Benmokrane, B. and Cousin, P. *ISIS Canada Research Network, Intelligent Sensing For Innovative Structures*. University of Sherbrooke GFRP Durability Study Report. University of Sherbrooke, Quebec, Canada, 2005.

Bakht, B., Tadros, G. and Brett, P. Report On The Studies Of GFRP Durability In Concrete From Field Demonstration Structures. *Journal for Composites in Construction.* 2005.

Brzev, S., Pao, J. (2006). "Reinforced Concrete Design ; A Practical Approach".*Pearsons Education.* Canada Inc., Toronto, Ontario, 2-3.

Bubani M, Soraru G, Tassone P. Mechanical durability of a polymer concrete: a Vickers indentation study of the strength degradation process. In: *Proceedings of 5th International Congress on Polymers in Concrete,* Honolulu, Hawaii; 2001.

Carreirra, D., & Chu, K. H. (1986). Stress-Strain Relationship for Reinforced Concrete in Tension. *Journal of the American Concrete Institute,*v 83 , n 1, 21-28.

CHBDC Candian Highway Bridge Design Code. (2006). Toronto: Canadian Standards Association International .

CHBDC Candian Highway Bridge Design Code. (2000). Toronto: Canadian Standards Association International .

Chu W., Wu L. and Karbhari V. Durability Evaluation of Moderate Temperature cured E-glass/ Vinylester Systems. *Composite Structures.* 2004; 1-4:367-376.

Collins, M., & Mitchell, D. (1997). *Prestressed Concrete Structures.* Response Publications.

CSA - S806-02, 2002. "Design and Construction of Building Components with Fibre-Reinforced Polymer". *Canadian Standard Association*, 178 Rexdale Boulivard, Toronto, Ontario, Canada M9W 1R3.

Davoudi, S. (2009). *CFRP Prestressed Concrete Prisms as Reinforcement in Continuous Concrete T-beams.* PhD disertation.Winnipeg: University of Manitoba.

de Scutter, G., Matthys, S., & Taerwe, L. (1997). *Two-Dimensional Analysis of Thermal Incompatability Between FRP Reinforcement and Concrete* . Proceedings of the Second International DIANA Conference on Finite Elements in Engineering and Science, (pp. 4-6). Amsterdam.

ISIS Canada Research Network, Intelligent Sensing For Innovative Structures. "Reinforcing *Structures with Fiber Reinforced polymers*." Design Manual 3. Winnipeg, Manitoba, Canada. 2001.

Fang, I. K., Worley, J. A., Burns, N. H., & Klinger, R. E. (1986). *Behaviour of Ontario type bridge deck on steel girders.* Research Report 350-1, Centre for Transpostration Research, Bureau of Engineering Research, The University of Texas Austin, Austin Tex.

Fields, K., & Bischoff, P. H. (2004). Tension Stiffening and Cracking of High Strength Reinforced Concrete Tension Members. *ACI Structural Journal*, 447-456.Is the name of this journal always capitalized?

Gilstrap, J., Burke, C., Dowden, D., & Dolan, C. (November 1997). Development of FRP Reinforcement Guidlines for Prestressed Concrete Structures. *Journal of Composites For Construction* , 131-135.

Hewitt, B. E., & Batchelor, B. d. (1975). Punching shear strength of restrained slabs. *ASCE Journal for Structural Division* , 101(ST0), 1827-1853.

Jackson, P. A., & Cope, R. J. (1990). The behaviour of deck slabs under full global loads. In author *Developments in Short and Medium Span Bridge Engineering* (Vol. 1, pp 253-264). Canadian Society for Civil Engineering.

Karbhari VM. Durability of FRP Composites for Civil Infrastructures Myth, Mystery or Reality. *Advances in Structureal Engineering.* 2003;6:3:243-256.

Leonhardt, F. (1964). *Prestressed Cooncrete - Design and Construction, English Translation.* Berlin: Wilhelm Ernst und Sohn.

Matsui, S., Tokia, D., Higashiyyama, H., & Mizukoshi, M. (2001). Fatigue Durability of fiber reinforced concrete deck slabs under running wheel loads. *Proceedings, Third International Conference under Severe Conditions*, (Vol 1, 982-991). Vancouver .

Memon, A.H. and Mufti, A.A. Fatigue Behavior of Second Generation Steel-Free Concrete Bridge Deck Slab, *Proceedings of the Second international Conference on FRP Composites in Civil Engineering (CICE 2004),* Adelaine , Australia, 2004.

Mufti, A. A., Bakht, B., & Jaeger, L. G. (1991). FRC Deck Slabs with Diminished Steel Reinforcement. *Proceedings, IABSE Symposium held in Leningrad* , 388-389.

Mufti, A. A., Jaeger, L. G., Bakht, B., & Wegner, L. D. (1993). Experimenetal investigation of FRC deck slabs without internal reinforcement. *Canadian Journal of Civil Engineering* , (20)3, 398-406.

Mufti, A., & Onofrei, M. (October 2004). *Long Term Performance of GFRP and Steel Anchor Assemblies for Markers in Concrete at Veteran Affairs - Brookside Cemetery.* Winnipeg, Canada: ISIS Canada Research Network.

Mufti, A.A., Onofrei, M., Benmokrane, B., Banthia, N., Boulfiza, M., Newhook, J.P., Bakht, B., Tadros, G. and Brett, P. Report On The Studies Of GFRP Durability In Concrete From Field Demonstration Structures. *Journal for Composites in Construction.* 2005.

Mufti, A., Memon, A. H., Bakht, B., & Banthia, N. (2002). Fatigue Investigation of Steel-Free Bridge Deck Slabs. *ACI International SP* , 61-70.

Newhook, J. P., & Mufti, A. A. (1996). A reinforcing steel-free concrete deck slab for the Solomon River Bridge. *Concrete International* , 18(6), 30-34.

Nkurunziza G, Debaiky A.S., Cousin P. and Benmokrane B. Durability of GFRP bars: A Critical Review of the literature. *Progress in Structural Engineering and Material.* 2005; 7:194-209.

OHBDC, 1979. " Ontario Highway Bridge Design Code." 1st Edition, Highway Engineering Division Ministry of Transportation, Downsview, Ontario, Canada.

Onofrei, M. *ISIS Canada Research Network, Intelligent Sensing For Innovative Structures*. Durability of GFRP Reinforced Concrete from field Demonstration Structures. University of Manitoba, Winnipeg, Canada, 2005.

Sen Rjan, Mullins, and Salem Tom. Durability of E-glass/ Vinylester Reinforcement in Alkaline Solution. *ACI Structural Journal.* 2002; 99:369-375.

Sheard, P. Clarke, J. L., Dill, M. Hammersely, G. and Ridchardson, D. EUROCONCRETE- taking account of durability for design of FRP reinforced concrete structures. *Nonmetallic (FRP) Reinforcement for Concrete Structures, Proceeding of 3 rd International Symposium. Sapporo. 1997;2:75-82.*

Sohanghpurwala, A. A. (June 2006). *Manual on Service Life of Corrosion - Damaged Reinforced Concrete Bridge Superstructure Elements.* Washington, DC: National Cooperatice Highway Research Program NCHRP Report 558.

Uomoto Taketo. Durability of FRP as Reinforcement for Concrete Structures. Advanced Composite Materials in Buildings and Structures 3rd International Conference. *Ottawa, Ontario, Canada, 2000, p 3-14.*

Vogel, H. (2005). *Thermal Compatability and Bond Strength of FRP Reinforcement in Prestressed Concrete Applications.* Master of Science disertation.Winnipeg: University of Manitoba.

Yi Chen, Davalos, and Indrajit Ray. Durability Prediction for GFR Bars Using Short-Tern Data Accelerated Aging Tests. *Journal for Composites for Construction.* 2006;10:279-286.